

# Application of Nanoparticles in the Diagnosis of Gastrointestinal Diseases: A Complete Future Perspective

Ning-ning Yue<sup>1</sup>, Hao-ming Xu<sup>2</sup>, Jing Xu<sup>2</sup>, Min-zheng Zhu<sup>3</sup>, Yuan Zhang<sup>4</sup>, Cheng-Mei Tian<sup>5</sup>, Yu-qiang Nie<sup>2</sup>, Jun Yao<sup>1</sup>, Yu-jie Liang<sup>6</sup>, De-feng Li<sup>1</sup>, Li-sheng Wang<sup>1</sup>

<sup>1</sup>Department of Gastroenterology, Shenzhen People's Hospital (the Second Clinical Medical College, Jinan University), Shenzhen, Guangdong, People's Republic of China; <sup>2</sup>Department of Gastroenterology and Hepatology, Guangzhou Digestive Disease Center, Guangzhou First People's Hospital, School of Medicine, South China University of Technology, Guangzhou, People's Republic of China; <sup>3</sup>Department of Gastroenterology and Hepatology, the Second Affiliated Hospital, School of Medicine, South China University of Technology, Guangzhou, Guangdong, People's Republic of China; <sup>4</sup>Department of Medical Administration, Huizhou Institute of Occupational Diseases Control and Prevention, Huizhou, Guangdong, People's Republic of China; <sup>5</sup>Department of Emergency, Shenzhen People's Hospital (the Second Clinical Medical College, Jinan University), Shenzhen, Guangdong, People's Republic of China; <sup>6</sup>Department of Child and Adolescent Psychiatry, Shenzhen Kangning Hospital, Shenzhen, Guangdong, People's Republic of China

Correspondence: De-feng Li; Li-sheng Wang, Department of Gastroenterology, Shenzhen People's Hospital (The Second Clinical Medical College, Jinan University; the First Affiliated Hospital, Southern University of Science and Technology), No. 1017, Dongmen North Road, Luohu District, Shenzhen, 518020, People's Republic of China, Tel +86 755 25533018, Email ldf830712@163.com; wanglsszrmyy@163.com

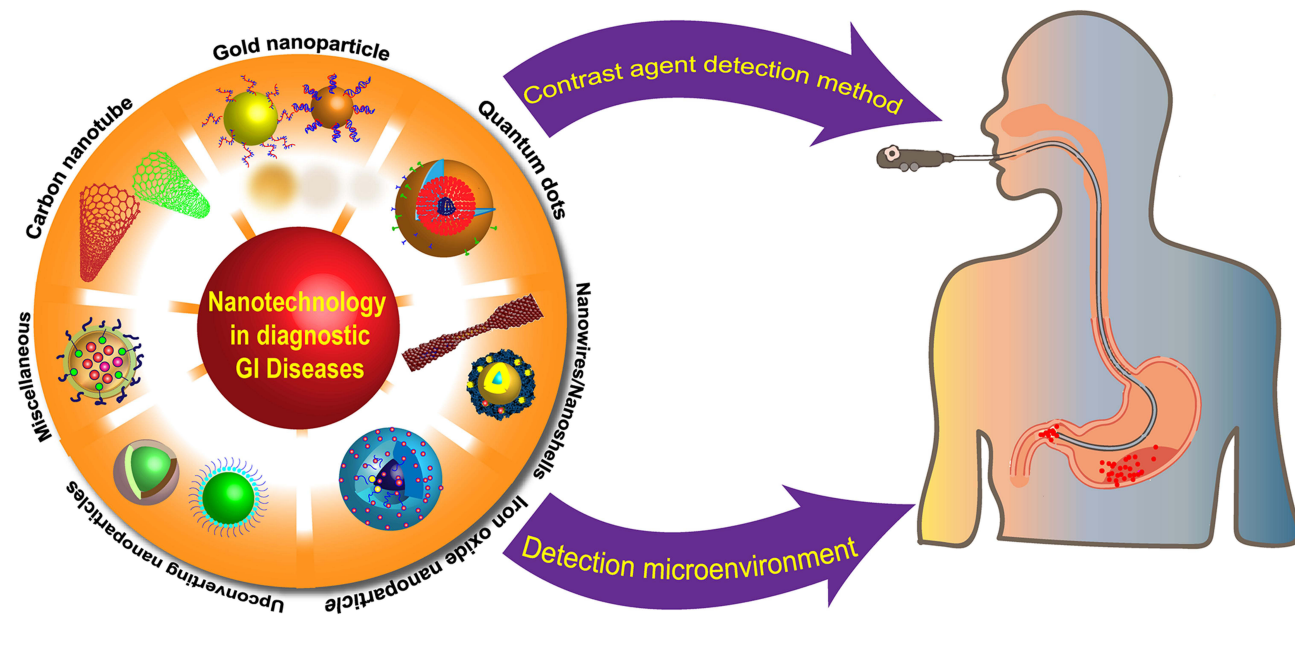
**Abstract:** The diagnosis of gastrointestinal (GI) diseases currently relies primarily on invasive procedures like digestive endoscopy. However, these procedures can cause discomfort, respiratory issues, and bacterial infections in patients, both during and after the examination. In recent years, nanomedicine has emerged as a promising field, providing significant advancements in diagnostic techniques. Nanoparticles, in particular, offer distinct advantages, such as high specificity and sensitivity in detecting GI diseases. Integration of nanoparticles with advanced imaging techniques, such as nuclear magnetic resonance, optical fluorescence imaging, tomography, and optical correlation tomography, has significantly enhanced the detection capabilities for GI tumors and inflammatory bowel disease (IBD). This synergy enables early diagnosis and precise staging of GI disorders. Among the nanoparticles investigated for clinical applications, superparamagnetic iron oxide, quantum dots, single carbon nanotubes, and nanocages have emerged as extensively studied and utilized agents. This review aimed to provide insights into the potential applications of nanoparticles in modern imaging techniques, with a specific focus on their role in facilitating early and specific diagnosis of a range of GI disorders, including IBD and colorectal cancer (CRC). Additionally, we discussed the challenges associated with the implementation of nanotechnology-based GI diagnostics and explored future prospects for translation in this promising field.

**Keywords:** nano-diagnostics, imaging, gastroenterology, gastrointestinal tumor, inflammatory bowel disease

## Introduction

Gastrointestinal (GI) diseases, which primarily encompass GI tumors and inflammatory bowel diseases (IBD), have a significant impact on the well-being of millions of people worldwide. Colorectal cancer (CRC) is the third most commonly diagnosed cancer, yet it ranks as the second leading cause of cancer-related deaths globally, posing a significant threat to human health.<sup>1</sup> Additionally, IBD is a chronic and recurrent inflammatory disorder that includes ulcerative colitis (UC) and Crohn's disease (CD). Its incidence exceeds 0.3%, substantially increasing the risk of CRC.<sup>2-4</sup> Given the absence of characteristic early symptoms in GI diseases, most patients are diagnosed at advanced stages, which severely affects their treatment options and overall prognosis. Consequently, the significance of early diagnosis cannot be overstated. Currently, the standard diagnostic tools for GI diseases consist of endoscopy, ultrasonography (US), computed tomography (CT), magnetic resonance imaging (MRI), and positron emission tomography (PET). Although endoscopy has improved diagnostic accuracy by enabling direct visualization of lesions, it is associated with various procedural complications, such as functional impairment, pain reactions, respiratory distress, and

## Graphical Abstract



bacterial infections, both during and after the invasive procedure.<sup>5</sup> Additionally, US, CT, MRI, and PET are commonly employed for staging comparison and surgical evaluation of GI diseases. However, due to the involuntary movement of the GI tract and the overlapping nature of abdominal tissues, their overall sensitivity in detecting GI diseases remains relatively low.<sup>6</sup> Moreover, their corresponding contrast agents lack targeted specificity, leading to nonspecific distribution, which can result in adverse effects, including allergic reactions, toxicities, and nausea. These limitations restrict their widespread clinical application. Therefore, there is an urgent need to develop innovative techniques, such as nanoparticle (NP)-based diagnostics, which offer high sensitivity and specificity, to overcome these challenges.

Nanotechnology involves the study of materials with structure sizes ranging from 1–100 nm, exploring their properties and potential applications. NPs exhibit a wide array of unique properties, such as optical, electrical, magnetic, thermal, and mechanical behaviors. Additionally, they possess advantages, such as a high surface-to-volume ratio, excellent biocompatibility, minimal toxicity, targeted capabilities, and the enhanced permeability and retention (EPR) effect. These characteristics make NPs highly promising for advancing disease diagnosis.<sup>7–9</sup> The combination of NPs with modern imaging techniques has been extensively investigated in various diseases, including tumors, cardiovascular disease, neurological disorders, liver disease, kidney disease, and more (Table 1)<sup>10,11</sup>. In recent years, NP-based imaging techniques have garnered significant attention in the diagnosis of GI diseases owing to their unique advantages.<sup>12</sup> This review aimed to provide a comprehensive overview of the different types of NPs and their properties as a foundation for nano-diagnostics. Subsequently, it focused on the applications and advancements of NP-based diagnostic approaches, in conjunction with modern imaging technologies, for the diagnosis of GI diseases. Finally, we delved into the challenges associated with nanotechnology-based GI diagnostics and discussed potential future directions for translation in this field.

## Key NPs in GI Diseases Imaging

NPs used for imaging GI diseases can be broadly classified into two categories based on their intrinsic properties: inorganic NPs and organic NPs. These NPs serve as imaging agents and nanocarriers, offering distinct functionalities in diagnostic applications.<sup>11,12,34</sup> These NPs vary in terms of their sizes, shapes, and properties, which consequently influence their specific applications in disease diagnosis. Therefore, it is crucial to have a comprehensive understanding

**Table 1** Commercialized NPs Have Been Explored as Contrast Agents for Molecular Imaging

NP Type	Targets	Imaging Modality	Animal Model	Outcome	Ref.
Quantum dots	Glucose transporter I (Glut I)	MRI	CRC-bearing mice	Specifically recognizing Glut I in CRC cells and improving the accuracy of CRC diagnosis and biopsy.	[13]
Superparamagnetic iron oxide NPs (SPIONPs)	Kupffer cells	MRI	Patients with hepatocellular carcinoma (HCC)	Improving the detection of HCC and the capacity to differentiate lesions.	[14]
Silica NPs	CD146	MRI/ Near-infrared fluorescence (NIRF)	MKN45 tumor-bearing nude mice	Allowing for rapid and accurate tumor imaging, with the potential to guide tumor treatment and surgery.	[15]
SPIONPs	Macrophages	MRI/PET/CT	IBD mice	Assessment of inflammatory activity in IBD.	[16]
CuS NPs	$\alpha\beta3$ / matrix metalloproteinase-2 (MMP-2)	MRI/NIRF	Gastric tumor-bearing mice	Accurate identification of gastric tumor.	[17]
Radiotracer-liposome	Esterase	PETCT	CT26 tumor-bearing mice	A pancreatic tumor a few millimeters in size is clearly visible.	[18]
Polymerized liposomal NPs	CA19-9	PET	Pancreatic cancer xenografts in mouse	Pancreatic cancer can be specifically recognized.	[19]
Copper NPs	CC chemokine Receptor 2(CCR2)	PET	Pancreatic ductal adenocarcinoma-bearing mouse	Pancreatic cancer can be detected with high sensitivity and accuracy.	[20]
Polymeric micellar NPs	EGFR	PET	CRC-bearing mouse	The PET imaging of CRC can be enhanced by active targeting.	[21]
Quantum dots	Large external antigen (LEA)	Fluorescence imaging	CRC-bearing mouse	Quantitative analysis of LEA expression in CRC.	[22]
Surface-enhanced Raman scattering NPs	EGFR /HER2	Endoscopy	Esophageal tumor-bearing mice	Visualization of esophageal tumor locations.	[23]
Fluorescent NPs	ASNYDA peptide	Confocal laser endomicroscopy	Barrett's esophageal adenocarcinoma-bearing rat	Specific identification of esophageal cancer.	[24]
Polymeric micelles	Glucose-regulated protein 78	SPECT/CT	Gastric cancer-bearing mice	The imaging of gastric cancer can be enhanced.	[25]
Fluorescent magnetic NPs	BRCAAI	Magnetofluorescent imaging	Gastric cancer-bearing mice	Early-stage gastric cancer can be recognized.	[26]
Ultrasmall SPIONPs	Peptide	MRI	HCC-bearing cancer	Early-stage HCC can be identified.	[27]
Upconversion NPs	Peptide	Upconversion luminescence (UCL)/ MRI	HCT116 tumor-bearing mice	Sensitive detection of ultra-small colorectal tumors.	[28]
68Ga-labeled Hepatitis E virus NPs	Integrin $\alpha3\beta1$	PET	HCT 116 CRC-bearing mice	Internalization of NPs in HCT116 cells is improved significantly, but the specific targeting efficiency needs to be further improved.	[29]
Fe <sub>3</sub> O <sub>4</sub> /Au/Ag NPs	Cytidine	SERS	Colon cancer-bearing mice	Detection of nucleoside concentrations at the nM level.	[30]
Human heavy-chain ferritin (HF <sub>n</sub> ) NPs	Transferrin receptor I (TfR1)	Endoscopy	Gastric cancer-bearing mice	Identification of early-stage gastric cancer.	[31]
Upconversion NPs	MGb2	MRI	Gastric cancer-bearing mice	Gastric cancer and adjacent lymphatic metastasis sites are detected ultra-sensitively by MRI.	[32]
Magnetic graphitic nanocapsules	Peptidoglycan	MRI	H. pylori-infected mice	H. pylori can be targeted for detection by MRI.	[33]

of the different types of NPs and their respective imaging mechanisms. This knowledge enables the flexible integration of modern imaging technologies, facilitating the generation of high-resolution images for the diagnosis of GI diseases.

## Nanowires (NWs)

NWs are one-dimensional structures with nanoscale cross-sections (<100 nm) and unlimited longitudinal lengths.<sup>35</sup> They can be categorized into various types based on their composition materials, including metal NWs (such as Ni, Ag, and Au),<sup>36,37</sup> semiconductor NWs (such as InP, Si, and GaN),<sup>38,39</sup> and insulator NWs (such as SiO<sub>2</sub> and ZnO).<sup>40</sup> Metal NWs, with their exceptional electrical,<sup>41</sup> optical,<sup>42</sup> thermal,<sup>43,44</sup> and mechanical properties,<sup>45,46</sup> have significantly impacted the field of bioimaging. For instance, copper NWs have been utilized in surface-enhanced Raman scattering (SERS) imaging, enabling signal amplification with remarkably high signal-to-noise ratio (SNR).<sup>47</sup> Magnetic NWs, serving as MRI contrast agents, have found increasing applications in the diagnosis of various diseases due to their customizable magnetic properties and favorable biocompatibility.<sup>48</sup> For example, iron-iron oxide core-shell NWs have demonstrated high efficiency in cell detection by acting as MRI T<sub>2</sub> contrast agents, promising to achieve the tracking of digestive tumor cells.<sup>48</sup> Silicon NW sensors offer numerous advantages in early disease diagnosis, providing rapid analysis of nanoscale sample volumes through resistance measurements.<sup>49</sup> For instance, Zheng et al have developed an antibody-functionalized silicon NW sensor that achieves ultra-sensitive detection of tumor markers in the concentration range of 50–100 fg/mL.<sup>50</sup> Additionally, Nami et al have employed a silicon NW biosensor to monitor T-cell counts and assess patients' immune responses by sensing pH changes in the extracellular environment caused by antigen-specific activated T-cell membrane acidification. This approach also holds promise for monitoring inflammatory responses in IBD.<sup>51</sup> Consequently, by combining different types of NWs with appropriate diagnostic technologies, significant advancements can be made in GI disease imaging, leading to improved diagnostic outcomes.

## Iron Oxide Nanoparticles (IONPs)

IONPs have garnered significant interest in bioimaging due to their exceptional magnetic properties and biocompatibility.<sup>52</sup> They serve as attractive contrast agents, effectively shortening the longitudinal and transverse relaxation time (T<sub>1</sub> and T<sub>2</sub>) to produce strong MRI contrast.<sup>53</sup> Furthermore, by integrating specific ligands, such as epithelial growth factor receptor (EGFR) antibodies, onto the surface of IONPs, molecular targeted MRI has been achieved for early detection of GI tumors, including gastric, pancreatic, colon, and hepatocellular carcinomas (Figure 1).<sup>54–56</sup> In addition to tumor diagnosis, IONPs hold considerable potential in the diagnosis of other digestive diseases. For example, single-nanometer IONPs coupled with type I collagen-binding peptides have been used as T<sub>1</sub>-weighted contrast agents to enhance liver imaging, enabling rapid and non-invasive diagnosis of liver fibrosis.<sup>57</sup> Superparamagnetic iron oxide nanoparticles (SPIONPs), a primary form of IONPs with a single-domain structure, exhibit superparamagnetic properties. Their paramagnetic magnetization under the influence of an external magnetic field is significantly higher than that of ordinary paramagnetic materials.<sup>58</sup> There has been increasing research on SPIONPs in the field of MRI, yielding exciting results. Chee et al have developed ultra-small SPIONPs coated

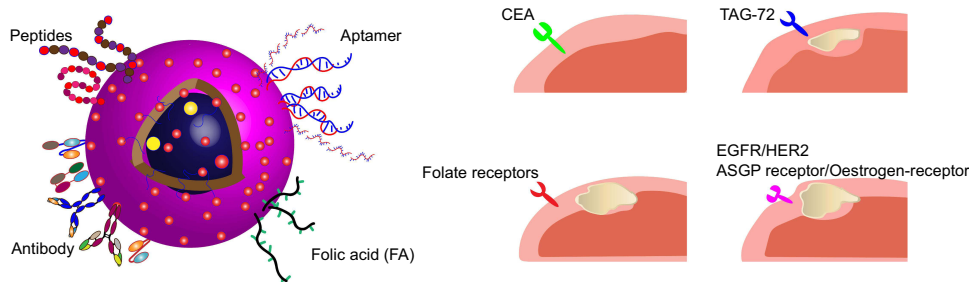


**Figure 1** Improving the imaging function by targeted nanoparticles. The common gastrointestinal tumor biomarkers overexpressed on cell membranes and the typical molecules/ligands used to modify the surface of nanoparticles for targeting imaging.

**Abbreviations:** CEA, carcinoembryonic antigen; TAG-72, tumor-associated glycoprotein-72; EGFR, epithelial growth factor receptor; HER2, human epidermal growth factor receptor 2; ASGP, asialoglycoprotein.<sup>50,61</sup>

with biocompatible peptides that specifically accumulate within liver tumors, thereby improving magnetic resonance properties and enabling specific detection of liver tumors as MRI T2 contrast agents.<sup>27</sup> Similarly, Yang et al have created an Alkyl-PEI-LAC-TPE/SPIO nano-complex as a dual-mode probe for MRI/optical imaging. This nano-complex effectively labels cancer cells and exhibits superior fluorescence properties and higher T2 relaxivity compared to the commercial contrast agent Feridex.<sup>59</sup> The remarkable magnetic properties of IONPs make them highly promising as MRI contrast agents in diagnostic applications, providing valuable insights into various GI diseases.

## Quantum Dots (QDs)

QDs are nanoscale spherical or sphere-like segments of semiconductor crystal materials with tunable optical properties, typically ranging from 2 to 10 nm in size. In QDs, the dimensions in all three directions are smaller than the Bohr radius of the exciton, which gives rise to unique optical characteristics.<sup>62–64</sup> Over the years, QDs have gained significant attention in the biomedical field due to their exceptional capabilities, including enhanced fluorescence stability and intensity (up to nearly 100 times brighter), high quantum yield, improved resistance to photobleaching, and high extinction coefficient.<sup>65,66</sup> QDs have been successfully employed for cell and protein labeling, enabling dynamic tracking of biological processes.<sup>67–69</sup>

Researchers have utilized the fluorescent properties of QDs to develop innovative diagnostic approaches. For example, Zhang et al have linked the fluorescent signal of QDs to the concentration of disease biomarkers by conjugating tyrosinase with detection antibodies. This fluorescence immunoassay enables the rapid detection of hepatocellular carcinoma (HCC) biomarker AFP at concentrations as low as 10 pM, offering a new avenue for early diagnosis and real-time monitoring of HCC.<sup>70</sup> Additionally, Deng et al have combined fluorescent and radioisotopic QDs with dextrose for targeting, tracking, and multimodal imaging of macrophages using PET/CT and fluorescence imaging. This approach contributes to the monitoring of immune responses in GI tumors and IBD.<sup>71</sup> Moreover, QDs show promise as contrast agents in medical imaging due to their small size, rapid clearance capability, and good biocompatibility. Notably, Dong et al have constructed ultrasmall Ag<sub>2</sub>Te QDs that exhibit negligible toxicity and excellent biocompatibility. These QDs are utilized for contrast-enhanced CT imaging due to their powerful X-ray attenuation capability.<sup>72</sup> Therefore, QDs hold great potential in advancing diagnostic techniques for digestive diseases, leveraging their fluorescence characteristics and X-ray attenuation capabilities for single-cell and molecular detection as well as deep-tissue imaging.

## Nanoshells

Nanoshells are ultra-thin metal shells that encase nanoscale cores of specific semiconductor complexes. They exhibit highly tunable optical characteristics, which depend on the thickness of the shell.<sup>73,74</sup> Given their plasmonic, optical, and thermal properties, nanoshells have found significant applications in various biomedical imaging techniques, including optical coherence tomography, diffuse optical tomography, US, PET, MRI, and SERS imaging.<sup>75–80</sup> One notable advantage of nanoshells is their ability to absorb or scatter near-infrared (NIR) wavelengths. By adjusting the thickness and size of the shells, their localized surface plasmon resonance (LSPR) can be tuned. This enables the NIR light to easily and deeply penetrate human tissue and blood, reaching depths of several centimeters. Furthermore, nanoshells can reduce the unwanted autofluorescence originating from substances like hemoglobin, lipids, and water.<sup>81,82</sup> For instance, silver nanoshells can be tailored into nanoprobe with high NIR activity by controlling their surface morphology. These nanoprobe exhibit strong and uniform SERS scattering signals in the NIR region and have been successfully utilized for detecting CRC.<sup>83</sup> Additionally, porous cubic AuAg nanoshells have been developed as NIR-II SERS probes, allowing the visualization of sub-millimeter microtumors in live mouse models.<sup>84</sup> Another advantage of nanoshells is their high loading capacity, particularly for hollow nanoshells. This feature enables precise control over the delivery of drugs, nucleic acids, contrast agents, and other biomolecules.<sup>85</sup> In a nutshell, the unique properties of nanoshells enhance the functionality of core NPs and hold great potential as nanoprobe for the early detection of GI tumors.

## Dendrimers

Dendrimers are nonpolymeric compounds with a three-dimensional, tree-like, globular structure. They are synthesized by adding highly branched layers to a central core.<sup>86</sup> These unique structures make dendrimers versatile platforms for various biomedical applications due to their cavities and easily modifiable surfaces.<sup>87,88</sup> Among dendrimers, polyamidoamine

(PAMAM) dendrimers have been extensively studied and characterized.<sup>89</sup> One notable application of PAMAM dendrimers is their use as carriers for delivering gadolinium ions in MRI. Markowicz-Piasecka et al have demonstrated that G4 PAMAM dendrimers can effectively increase signal intensity in the liver by 59–116% after administering gadolinium-based compounds, providing enhanced MRI contrast.<sup>90</sup> Unlike other NPs, dendrimers offer a tunable molecular structure, narrow polydispersity index, a large number of terminal functional groups, and available interior cavities and branches.<sup>91</sup> These features allow specific molecular targets associated with diseases to bind to the terminal functional groups, making dendrimers “smart” and capable of precise targeting of cancers or other disorders. For example, Li et al have developed a dual-mode nanoprobe targeting the urokinase-type plasminogen activator receptor (uPAR) using dendritic grafted polylysine (DGL)-U11. This nanoprobe is loaded with the MRI contrast agent  $Gd^{3+}$  and the NIR fluorescent cyanine dye Cy5.5 for ultra-early detection of pancreatic cancer. The targeted nanoprobe improves the sensitivity and spatial resolution of MRI/near-infrared fluorescence (NIRF) imaging, offering a promising nanoplatform for the early detection of pancreatic cancer.<sup>92</sup> Therefore, the specific targeting capabilities of dendrimers, combined with the EPR effect, enable them to serve as carriers for contrast agents, promoting the applications of MRI, CT, PET, and optical imaging in the diagnosis of digestive diseases.<sup>90,93–95</sup>

## Carbon Nanotubes (CNTs)

CNTs are nanoscale cylindrical tubes rolled from graphene sheets. They can be classified into single-walled carbon nanotubes (SWCNTs) with diameters of about 1–2 nm and multi-walled carbon nanotubes (MWCNTs) with diameters ranging from 10–100 nm. MWCNTs consist of 2–30 concentric SWCNTs.<sup>96</sup> In biomedical imaging, SWCNTs are preferred over MWCNTs due to their ability to emit NIRF that is environmentally sensitive to factors, such as pH and ionic strength.<sup>97–99</sup> Consequently, SWCNTs are often used as fluorescent probes either because of their intrinsic optical properties or their capacity to label fluorescent molecules.<sup>100</sup> Researchers have explored the use of SWCNTs as NIRF agents for dynamic contrast-enhanced imaging. Welsher et al have utilized SWCNTs as NIR-II fluorescent agents and observed significant improvement in the anatomical resolution of organs over time. This represents a promising approach for achieving high-resolution optical imaging through deep soft tissues in the abdomen.<sup>101</sup> Additionally, the superior biocompatibility and ease of surface functionalization of CNTs make them potential carriers for contrast agents. Rivera et al have encapsulated bismuth in SWCNTs bound to pig bone marrow-derived mesenchymal stem cells, resulting in increased contrast in CT imaging and negligible cytotoxicity compared to control cells.<sup>102</sup> By harnessing their fluorescent and contrast agent loading capabilities, these CNTs can achieve higher-resolution imaging of digestive diseases, enabling enhanced visualization and detection of GI conditions.

## Gold Nanoparticles (AuNPs)

AuNPs have garnered significant attention as promising contrast agents and are extensively studied in biomedical imaging applications.<sup>103</sup> AuNPs exhibit unique properties at the nanoscale, including tunable physical, chemical, and biological characteristics.<sup>104</sup> They can take on various shapes and sizes, such as nanorods, nanospheres, nanotriangles, nanostars, nanocubes, nanoshells, nanohexagons, nanoclusters, nanobranched structures, and hollow spheres.<sup>105</sup> With their non-toxicity and biocompatibility, AuNPs have emerged as versatile tools in biomedical imaging techniques, including cell imaging, optical imaging (such as optical coherence tomography,<sup>106</sup> narrow-band imaging,<sup>107</sup> and dark field microscopy<sup>108</sup>), and CT.<sup>109</sup>

AuNPs can serve as NIR-active probes because their LSPR wavelength can be tuned to NIR light, allowing for deep-tissue penetration. For instance, NIR-emitting AuNPs conjugated to the mechano-growth factor (MGF) are utilized for fluorescent imaging to detect its expression in CRC.<sup>110</sup> Moreover, AuNPs can be employed in disease diagnosis using the SERS technique, which amplifies the Raman signal when the analyte interacts with the surface plasmas of AuNPs. This technique enables highly sensitive and label-free detection of specific analytes. Aptamer-functionalized AuNPs have been used as SERS biosensors to quantitatively detect IL-6, a cytokine associated with inflammation and cancer progression, offering the potential for monitoring immune responses in GI tumors and IBD.<sup>111</sup> Additionally, AuNPs have been investigated as contrast agents for cell tracking and CT imaging due to their high X-ray absorption coefficient.<sup>112</sup> By labeling T cells expressing tumor-specific receptors with AuNPs, Meir et al have demonstrated the accumulation of these

T cells at tumor sites using whole-body CT imaging, providing a valuable tool for the diagnosis and monitoring of digestive diseases.<sup>112</sup> In summary, AuNPs exhibit diverse properties that make them attractive contrast agents in various imaging modalities, including fluorescent imaging, SERS-based detection, and CT imaging. Their tunable properties, biocompatibility, and versatility contribute to their potential in the diagnosis, monitoring, and characterization of digestive diseases.

## Miscellaneous NPs

### Polyelectrolyte Complex Nanoparticles (PECNPs)

PECNPs are formed by mixing polymers with opposite charges in aqueous solutions, and they can be any charged substances, like surfactants, proteins, and colloids.<sup>113–116</sup> The formation of PECNPs relies on electrostatic interactions, polymer size, mixing order, mixing ratio, polymer concentration, and pH conditions.<sup>117,118</sup> These complexes possess desirable properties, such as a high surface-to-volume ratio, good tolerability, biocompatibility, and sensitivity to pH, allowing for the controlled release of loaded substances.<sup>119–121</sup> PECNPs have been extensively explored for biomedical imaging purposes. For example, they have been utilized for the protection, delivery, and imaging of curative proteins by loading them with upconversion nanoparticles (UCNPs).<sup>122</sup> PECNPs have also been employed as carriers for contrast agents in imaging applications.<sup>123</sup> Gadolinium-loaded PECNPs, for instance, have been prepared for enhanced MRI.<sup>124</sup> Similarly, PECNPs complexed with SPIONPs have demonstrated improved MRI contrast compared to SPIONPs alone.<sup>125</sup> These NPs offer a versatile platform for delivering contrast agents to specific locations, enabling accurate and targeted imaging of GI diseases.

### Calcium Phosphate Nanoparticles (CaPNPs)

CaPNPs have garnered attention in the field of biomedical imaging due to their similarities to the major inorganic components of natural bone and teeth.<sup>126</sup> These NPs offer several advantages, including biocompatibility and eosinophilic degradation.<sup>127–130</sup> CaPNPs have been employed as versatile tools for various applications, including drug delivery,<sup>128</sup> gene delivery,<sup>131</sup> and vaccine adjuvants.<sup>132</sup> Additionally, they can serve as carriers for contrast agents in biomedical imaging. For example, gadolinium-loaded CaPNPs have been developed, exhibiting higher longitudinal relaxivity and longer imaging time compared to gadolinium alone.<sup>133</sup> Another study by Mi et al has reported the use of pH-sensitive CaPNPs with a poly(ethylene glycol) shell as an MRI contrast agent. Under low pH conditions, the CaPNPs would decompose and release  $Mn^{2+}$ , selectively enhancing the MRI contrast of HCC.<sup>134</sup> By utilizing their transport capacity, CaPNPs can effectively contribute to the imaging of GI diseases. These NPs provide a platform for delivering contrast agents to specific locations, enabling enhanced imaging and diagnosis of GI disorders.

### Perfluorocarbon Nanoparticles (PFCNPs)

PFCNPs are versatile nanomaterials that offer numerous advantages. They exhibit high chemical inertness, low diffusivity, and low solubility, and are non-toxic, while also being resistant to degradation.<sup>135</sup> By subjecting PFCNPs to ultrasonic treatment, they can be converted into microbubbles, leading to effective intra-tumor aggregation and enhanced ultrasound imaging. This addresses the issue of short retention time typically observed with micron-sized microbubbles in tumors.<sup>136</sup> For instance, Koshkina et al have developed perfluoro-15-crown-5-ether-loaded poly(lactic-co-glycolic acid) NPs, which significantly improve ultrasound contrast during repeated imaging sessions over a 48-hour period.<sup>137</sup> Moreover, PFCNPs generate a  $^{19}F$  signal that offers higher sensitivity and resolution compared to other MR-receptive nuclei.<sup>135</sup> For instance, Shin et al have employed  $^{19}F$  MRI to evaluate the severity of IBD by labeling macrophages. Their study demonstrates a positive correlation between local  $^{19}F$  signal intensity and the degree of colitis inflammation.<sup>138</sup>

### Liposomes

Liposomes are spherical vesicles composed of a lipophilic bilayer that encloses an aqueous core.<sup>139</sup> They offer unique advantages as drug delivery systems, including biocompatibility, biodegradability, ease of surface modification, and high loading capacity.<sup>140–143</sup> By engineering their composition, size, and surface charge, liposomes can be tailored for biomedical imaging applications.<sup>144</sup> For instance, Thébault et al have developed liposomes encapsulating magnetic NPs (maghemite,  $\gamma-Fe_2O_3$ ) to enhance MRI contrast.<sup>145</sup> Awad et al have designed stealth liposomes coated with hydrophilic graphene QDs for effective delivery to CRC tissues while reducing systemic toxicity.<sup>146</sup> Additionally, radiolabeled liposomes have also been utilized in PET

imaging.<sup>147</sup> Technetium-99m-labeled polyethylene glycol (PEG)-liposomes demonstrate rapid imaging of IBD in a rabbit model of acute colitis.<sup>148</sup> Furthermore, Blocker et al have successfully utilized <sup>64</sup>Cu-labeled liposomes to localize CRC.<sup>149</sup> Liposomes as nanocarriers of imaging agents hold great potential for the diagnosis of GI diseases.

### Micelles

Micelles are self-assembled agglomerates with hydrophobic cores and hydrophilic shells formed in an aqueous environment.<sup>150</sup> They possess several key properties, including high stability, excellent biocompatibility, prolonged circulation time, and the EPR effect.<sup>151–153</sup> Additionally, their ability to effectively solubilize poorly soluble drugs and target specific areas makes them highly desirable for biomedical applications.<sup>25,154</sup> The amphiphilic nature of micelles makes them attractive as carriers for contrast agents in biomedical imaging.<sup>155</sup> For example, surfactant-stripped frozen pheophytin micelles have been successfully prepared and utilized for multimodal imaging of the gut using fluorescence, photoacoustic, and PET techniques.<sup>156</sup> Cheng et al have developed <sup>111</sup>In-labeled micelles guided by glucose-regulated protein 78 binding peptides, which increase radioactivity and accumulation of <sup>111</sup>In in gastric tumors for nuclear imaging.<sup>25</sup> Moreover, Jiang et al have encapsulated aggregation-induced luminophores in micelles, enabling high-resolution fluorescence and photoacoustic imaging of the gut.<sup>157</sup> Hence, loading different contrast agents into micelles offers a promising “two birds with one stone” imaging approach for the diagnosis of digestive diseases.

### UCNPs

UCNPs are a unique class of photosensitive materials capable of converting low-energy photons into high-energy photons upon excitation by NIR light sources.<sup>158</sup> This phenomenon, known as the anti-Stokes shift, allows the transformation of NIR light into ultraviolet and visible light through nonlinear optical processes.<sup>159</sup> Typically, UCNPs consist of an inorganic matrix, sensitizer, and activator (usually rare earth-doped ions).<sup>160</sup> Sensitizer ions, such as doped Ln<sup>3+</sup> ions, absorb NIR photons and transfer the energy to the activator ions, typically Yb<sup>3+</sup>, through sequential energy transfer processes. The excited activator ions then emit photons, resulting in fluorescence.<sup>161,162</sup> UCNPs possess several advantages over organic dyes or fluorescent proteins. They exhibit nonblinking behavior, are not prone to photobleaching, and do not suffer from background fluorescence interference. Additionally, UCNPs offer high chemical stability, narrow emission bands, and large anti-Stokes emission, making them highly desirable for diagnostic applications in GI diseases.<sup>163–167</sup> Compared to QDs, UCNPs possess lower toxicity, higher SNR, and longer lifetime.<sup>168</sup> These exceptional properties have positioned UCNPs at the forefront of GI disease diagnostics. For instance, Qiao et al have utilized UCNPs as a unique probe for the sensitive detection of primary gastric tumors and lymphatic metastasis through upconversion luminescence (UCL) imaging.<sup>32</sup> Tian et al have successfully developed a novel contrast agent, lanthanide-doped UCNP-Ulex Europaeus Agglutinin-I, which exhibits high tumor-targeting capacity and enables deep-tissue imaging in a mouse model of CRC.<sup>169</sup> Furthermore, Chu et al have established a UCL system based on UCNPs for rapid and accurate quantification of IL-6, offering the potential for early diagnosis of inflammatory GI diseases.<sup>170</sup> Thus, UCNP-based luminescence imaging utilizing the “optical window” provided by UCNPs holds great promise for effective imaging of GI diseases.

## Nanotechnology in the Diagnostic Applications of GI Diseases

Currently, clinical diagnosis of digestive diseases relies on various imaging technologies, including endoscopy, CT, MRI, US, PET, and single photon emission computed tomography (SPECT). However, each of these techniques has its own advantages and limitations, and these limitations can pose significant challenges in clinical diagnosis.<sup>87</sup> In order to overcome these challenges, NPs have been introduced, leveraging their unique physical and chemical properties to achieve high sensitivity, high resolution, safety, and the ability to provide detailed anatomical and biological information about specific target sites. In the following sections, we summarized the progress of several NP-based imaging techniques in the context of digestive diseases (Table 2).



**Table 2** NP Based Diagnostic Tests for GI Disorders

NP	GI Disease Type	Imaging	Comment	Ref.
Near-infrared fluorescent silica NPs	CRC	Endoscopy	Early-stage CRC(<0.5mm <sup>2</sup> ) can be detected and depicted in human-scale animal model, which offers a viable pathway for clinical translation for primary CRC detection.	[171]
Anti-CEA loaded maghemite NPs	CRC	SERS	CEA-expressing cells can be identified with high specificity in vitro, providing a potential detection tool for CEA-expressing tumors, micrometastasis, and cancer-circulating cells.	[172]
Carbon NPs	CRC	Laparoscopy	Effective and safe detection of CRC and tracking of lymph nodes is achieved during laparoscopic surgery for CRC.	[173]
AuNPs	CRC	SERS	Non-invasive detection of CRC with high specificity and sensitivity in serum samples.	[174]
UCNPs	CRC	Dual-mode UCL/MRI	Ability to target and detect ultra-small colorectal tumors.	[28]
Gadolinium-loaded solid lipid NPs	CRC	MRI	The NP-based contrast agent can be effectively absorbed by CRC cells to enhance MRI in colorectal tumors.	[175]
QDs	Colon cancer	Endoscopy	Providing an approach for detecting small and flat tumors and improving cancer diagnosis.	[176]
Near-infrared fluorescent proteinoid-poly (L-Lactic Acid) hollow NPs	Colon cancer	NIRF	The hollow NPs are used for the encapsulation of the NIR dye indocyanine green, increasing significantly the photostability of the dye and conjugating with tumor-targeting ligands for specific colon tumor detection.	[177]
Raman scattering NPs	GI cancers	Raman endoscopy	Small precancerous lesions can be detected in animal models, which provides earlier detection method for esophageal, gastric, and colorectal tumors.	[178]
Peptide-coated ultrasmall SIONPs	Liver tumors	MRI	The contrast of MRI in early-stage liver tumors is enhanced.	[27]
Iodinated liposomes	Hepatic tumors	CT	Small liver metastases and vessels can be detected by enhanced CT.	[179]
Lactobionic acid-modified dendrimer-entrapped AuNPs	HCC	CT	HCC can be diagnosed by targeted CT imaging in vivo and in vitro.	[180]
Acetylated polyethylenimine-entrapped AuNPs	HCC	CT	Highly improving the CT contrast enhancement of normal liver and as an effective negative CT contrast agent for diagnosing HCC.	[181]
IONPs	Liver tumors	MRI	Liver tumors can be detected by targeted MRI with ultralow hepatotoxicity.	[182]
Bismuth-based nanoprobe	Liver fibrosis	Spectral CT	Optimizing the prominence of the lesion area and successfully differentiating liver fibrosis from the healthy liver.	[183]
Rhenium sulfide (ReS <sub>2</sub> ) NPs	GI tract	Spectral CT	GI tract can be depicted obviously by spectral CT.	[184]
Nanobubbles	Gastric cancer	US	Nanobubbles are able to pass through the vascular for extravascular ultrasound imaging of tumors in the gastric cancer xenografts.	[185]
Multicolour carbon dots (CDs)	Pancreatic cancer	Fluorescence imaging	CDs can effectively accumulate at tumor site in a murine model of pancreatic cancer and demonstrate excellent fluorescence imaging capabilities, contributing to accurate resection of tumors.	[186]
Copper NPs	Pancreatic ductal adenocarcinoma (PDAC)	PET	<sup>64</sup> Cu-radiolabeled nanovehicle allows sensitive and accurate detection of PDAC malignancy by PET imaging in mouse models.	[20]
Dextran-coated cerium oxide NPs (Dex-CeNPs)	IBD	CT	Dex-CeNPs accumulate in the colitis area, producing enhanced CT contrast.	[187]
Lanthanide-doped nanocrystals	IBD	NIRF	Providing a real-time 3D imaging of the GI tract in mice.	[188]

## Endoscopy NIRF Imaging

Endoscopy is a commonly used diagnostic tool for GI diseases and plays a crucial role in the early detection of GI tumors and assessment of mucosal inflammation, leading to a reduction in morbidity and mortality. While white light endoscopy (WLE) can easily detect polypoid lesions, there is a significant miss rate for potentially invasive flat or depressed lesions. For example, the miss rate for flat adenomas is reported to be 34%, while for flat adenomas, it is as high as 42%.<sup>189</sup> To overcome these challenges, new high-resolution imaging techniques for GI endoscopy have emerged, particularly those incorporating optical techniques, such as chromoendoscopy, narrow-band imaging, autofluorescence imaging, Raman spectroscopy, blue laser image, confocal laser endomicroscopy, and NIRF imaging.<sup>190,191</sup> These techniques have significantly improved the early diagnosis of GI tumors. NIRF imaging involves the use of a photo-detection device to capture fluorescent signals generated by either endogenous fluorescent molecules or exogenous molecular probes. The captured signals are then processed and analyzed by a computer to construct high-resolution images.<sup>192</sup> NIRF imaging offers several advantages, including non-invasiveness, real-time imaging, absence of radiation, high sensitivity, and the ability to detect multiple signals.<sup>193</sup> One of the key advantages of NIRF imaging is its capability to work in the NIR region (650–900 nm), where biological tissues exhibit minimal light absorption and scattering effects. Additionally, the background fluorescence of tissues in this region is low, resulting in a high SNR and enhanced tissue penetration capability.<sup>194–196</sup> NIRF imaging has been successfully employed in tumor staging and image-guided tumor resection, enabling real-time and high-resolution identification of tumor margins during surgery.<sup>60</sup> It has proven to be a valuable tool in improving the accuracy of surgical procedures.

Indocyanine green, a NIR fluorescent dye, is one of the most widely used imaging probes approved by the USA Food and Drug Administration. It has found applications in various clinical practices, such as liver and cardiac function assessment and retinal angiography.<sup>197,198</sup> However, there are several limitations associated with indocyanine green that hinder its broader use in disease diagnosis. These limitations include its short half-life, the tendency to aggregate undesirably, poor hydrolytic stability, limited photostability, nonspecific targeting, and inadequate deep-tissue imaging capabilities.<sup>199,200</sup> In contrast, NP-based probes offer several advantages that overcome these limitations. They provide high optical intensity and stability, large payloads, low self-aggregation, enhanced biocompatibility, multimodal signaling capabilities, target binding through the EPR effect or multiple ligands, and adjustable biodistribution profiles. These characteristics assist in the identification of early and relatively small lesions.<sup>201,202</sup> Tiernan et al have developed a fluorescent contrast agent by conjugating dye-doped silica NPs with anti-CEA antibodies, which enhances the imaging of colorectal tumors and shows great potential in intra-operative fluorescent visualization of tumor cells.<sup>203</sup> Furthermore, Xu et al have designed a novel activatable nanoprobe by encapsulating H<sub>2</sub>S-activatable fluorescent probes inside the hydrophobic interior of core-shell silica nanocomposites. NIRF imaging demonstrates that this probe enables deep-tissue imaging of CRC.<sup>204</sup>

While NIRF imaging offers many advantages, it does have limitations in terms of tissue penetration, particularly for the diagnosis of GI diseases. As a result, its applicability is most significant in endoscopy of digestive disorders, where it can directly visualize abnormal mucosa and organs. For instance, Park et al have developed a rapid and accurate fluorescence imaging technique using antibody-coated QDs to spray and wash CRC tissue in living animals, followed by excitation and imaging through an endoscope. This nanoprobe enables the diagnosis of tumors in less than 30 minutes and provides imaging at a depth of 100 microns, allowing the detection of small or flat tumors that may be missed by WLE.<sup>176</sup> Gournaris et al have utilized inflammatory macrophage-targeted gold nanorods labeled with Cy5.5 for endoscopic NIRF imaging of CRC. This approach successfully detects inflammatory bowel polyps and enables their precise ablation using radiofrequency, demonstrating promise for both CRC detection and the treatment of various inflammatory diseases.<sup>205</sup> Furthermore, Rogalla et al have designed and evaluated a biodegradable NIRF silica nanoprobe. With the assistance of this fluorescent nanoprobe, WLE can detect and characterize colorectal adenomas smaller than 5 mm<sup>2</sup>, offering the potential for early detection of CRC in high-risk patients.<sup>171</sup> Therefore, the use of NP-based NIRF imaging with improved tissue penetration significantly enhances the diagnostic accuracy of endoscopy. However, it is important to consider the accurate targeting of the nanoprobe to the specific site of interest. While the deposition of NPs at lesion sites based on the EPR effect is not entirely specific, the development of tumor-specific molecular nanoprobe holds promise for further advancements in this field.

## CT

CT, a non-invasive and convenient diagnostic tool, is widely used in clinical practice. It involves rotating an X-ray source around the scanned object to obtain detailed images. X-rays possess excellent deep-tissue penetration ability, high spatial resolution, and fast scanning speed, and they allow for painless examination and easy image processing. These features make CT imaging an attractive technology for the diagnosis of GI diseases.<sup>206</sup> To improve the distinction between different tissue types, contrast agents are commonly used.<sup>207</sup> Water-soluble aromatic iodinated molecules and barium sulfate suspensions are the primary contrast agents employed for enhanced CT imaging. Barium sulfate is primarily administered orally for GI imaging due to the toxicity associated with barium ions. However, it has limitations in terms of its use and cannot be administered intravenously. On the other hand, iodine-based agents, which have a high absorption coefficient for X-rays, are generally safe for intravascular administration. However, they are rapidly cleared from the kidneys due to their short circulation time in the body after administration. Furthermore, patients may experience varying degrees of adverse reactions, such as dizziness, vomiting, or skin irritation, due to the high osmotic pressure and viscosity of these agents. Additionally, these contrast agents lack tissue or organ targeting and specific biodistribution, resulting in limited specificity in imaging applications.<sup>208,209</sup>

Indeed, the development of novel contrast agents based on NPs has gained significant attention for CT imaging. NPs offer several advantages, such as a large surface area, enhanced stability, prolonged circulation time, superior biocompatibility, specific targeting, and low toxicity, making them well-suited for CT imaging applications (Figure 2).<sup>210-213</sup> There are various types of NP-based contrast agents under development, including iodine-based agents (such as liposomes, micelles, polymers, and dendrimers), AuNPs, lanthanide-based NPs (such as macromolecules or emulsions containing

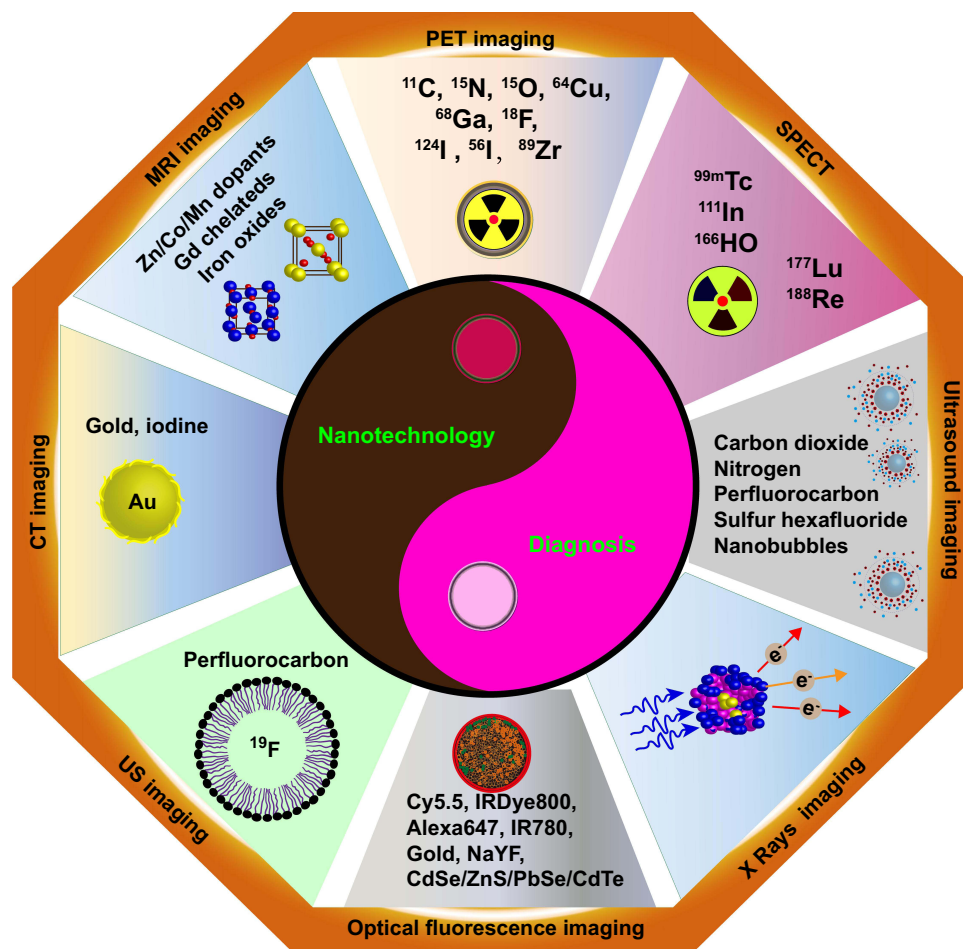


**Figure 2** Nanoparticle combined with imaging technique for diagnostic of gastrointestinal disorder.<sup>219</sup>

lanthanides and UCNPs), and other heavy metal-based contrast agents (such as tantalum or bismuth).<sup>214,215</sup> In the case of iodine-based contrast agents, small iodinated molecules can be encapsulated or conjugated within nanocarriers to extend their circulation time and enhance the sensitivity of CT imaging.<sup>216,217</sup> For example, Montet et al have utilized iodinated liposomes to improve the sensitivity of detecting liver metastases by enhancing vascular and hepatic CT imaging. The iodinated liposomes, taken up by Kupffer cells in the liver instead of being rapidly excreted by the kidneys, amplify the contrast enhancement in the liver, enabling the detection of small liver metastases.<sup>179</sup> Similarly, iodinated dendrimers have been employed as blood-pool contrast agents, overcoming the rapid renal excretion of small iodinated compounds and reducing their side effects. Dendritic contrast agents have demonstrated high contrast enhancement and prolonged enhancement time in the blood pool, facilitating the diagnosis of tumors through the EPR effect.<sup>218</sup> However, encapsulating water-soluble ionic or nonionic iodinated molecules within micelles solely through hydrophobic interactions can be challenging. The covalent attachment of iodinated contrast media to the hydrophobic tails of amphiphiles, followed by incorporation into the core of micelles, has been a key method for preparing iodinated micelles. These iodinated micelles serve as CT contrast agents, offering the potential for long-lasting blood-pool contrast and enhanced imaging.<sup>217</sup>

Furthermore, AuNPs serve as excellent contrast agents in CT imaging due to their high X-ray attenuation and ease of surface functionalization.<sup>180,220</sup> Zhou et al have successfully enhanced the CT contrast of normal liver and weakened it in hepatic necrotic areas by entrapping AuNPs with acetylated polyethyleneimine, achieving effective negative contrast in CT.<sup>181</sup> In recent years, bismuth-based NPs have emerged as highly promising contrast agents for imaging GI diseases owing to their high X-ray absorption and biosafety.<sup>221,222</sup> Zelepukin et al have designed polymer-coated bismuth oxychloride nanosheets for CT imaging of colitis in animals, resulting in a 2.55-fold enhancement in contrast with lower toxicity compared to conventional contrast agents.<sup>223</sup> Furthermore, lanthanide-based NPs are also being explored as contrast agents in CT. Naha et al have developed dextran-coated cerium oxide NPs (Dex-CeNPs) for CT imaging of IBD in a mouse model, which significantly improves CT imaging by accumulating in colitis areas. Additionally, more than 97% of Dex-CeNPs are cleared from the body within 24 hours, demonstrating a favorable biosafety profile.<sup>187</sup>

Moreover, spectral CT imaging technology, which utilizes the differential absorption of tissues at different energy levels of X-rays, offers effective tissue distinction and reduces image artifacts.<sup>224,225</sup> NP-based spectral CT can enhance the imaging of microscopic lesions, particularly aiding in qualitative analysis and identification of upper abdominal diseases. For example, Wu et al have reported the successful diagnosis of liver fibrosis using a bismuth-based nanoprobe with high efficacy.<sup>183</sup> Additionally, Wang et al have prepared rhenium sulfide (ReS<sub>2</sub>) NPs that significantly improve contrast in spectral CT imaging of the GI tract, demonstrating minimal toxicity.<sup>184</sup> Overall, NP-based CT imaging technology holds great promise for the diagnosis of digestive diseases.

## MRI

MRI has extensive clinical applicability in diagnosing GI diseases due to its non-invasive and non-ionizing radiation, excellent spatiotemporal resolution, accurate soft tissue contrast, and deep-tissue penetration.<sup>226</sup> Protons within the body are excited by RF pulse energy in a magnetic field and emit radio waves, which are then processed by a computer to construct clear structural images.<sup>227</sup> While gadolinium complex is a widely used T1 contrast agent in clinical practice, providing positive contrast in MRI by shortening the longitudinal relaxation time of surrounding water molecules, its retention in GI tissues for an extended period is challenging due to the empty nature and involuntary movement of abdominal organs.<sup>61</sup> Furthermore, short circulation time, nonspecific distribution, poor detection sensitivity, and toxicity issues associated with gadolinium complex further restrict their clinical application.<sup>228–230</sup> NP-based contrast agents offer a promising platform for MRI diagnostics due to their unique advantages. On the one hand, NPs have a high payload capacity, allowing for enhanced imaging contrast at low doses of contrast agents.<sup>231</sup> On the other hand, NPs with a large surface-to-volume ratio enable multi-modality MRI by facile surface modifications (eg, targeting with antibodies or peptides) or the introduction of additional features (eg, fluorescence).<sup>232,233</sup> Based on the mechanism of contrast enhancement, NP-based MRI contrast agents can be classified into T1 contrast agents and T2 contrast agents. Gadolinium-based NPs (such as dendrimers,<sup>234</sup> liposomes,<sup>235</sup> micelles,<sup>236</sup> QDs,<sup>237</sup> silica,<sup>238</sup> and CNTs<sup>239</sup>) serve as promising T1 contrast agents, offering positive contrast enhancement. In an early study, Kobayashi et al have synthesized a unique MRI contrast agent by loading gadolinium-diethylenetriaminepentaacetic acid (Gd-DTPA) onto polypropylene-diaminobutane dendrimers for the diagnosis of liver micrometastases. The nano-contrast agent uniformly enhances normal liver parenchyma and

accurately visualizes micrometastases as small as 0.3 mm in diameter in the mouse liver.<sup>240</sup> Furthermore, dendrimers targeting endothelin (which is enriched at the HCC margin) loaded with Gd-DTPA and the NIR fluorophore IR783 have demonstrated the ability to clearly delineate tumor boundaries. After 30 minutes of injection, this complex enables successful visualization of tumors as small as 1–4 mm in diameter, offering a promising non-invasive and precise preoperative definition of tumor margins and intraoperative guidance for tumor resection using NIRF imaging.<sup>241</sup> Similarly, Wang et al have utilized solid-lipid nanoparticles (SLNs) loaded with both Gd-DTPA and fluorescein isothiocyanate (FITC) as MRI contrast agents for diagnosing CRC. The Gd-FITC-SLNs exhibit significantly increased SNR and circulation time, resulting in the durable enhancement of CRC.<sup>242</sup> Additionally, Pagoto et al have developed vascular cell adhesion molecule-1 receptor-targeted phospholipid-based micelles loaded with Gd-DOTA for MRI visualization of inflammatory sites. This micellar system exhibits good biocompatibility, high longitudinal relaxation, and an improved ability to detect areas of inflammation by enhancing MRI T1 contrast. It holds promise for early MRI diagnosis of inflammatory diseases of the GI tract.<sup>236</sup>

In recent years, there has been significant interest in manganese oxide NPs (such as MnO, MnO<sub>2</sub>, Mn<sub>2</sub>O<sub>3</sub>, Mn<sub>3</sub>O<sub>4</sub>, and MnO<sub>x</sub>) as contrast agents for MRI T1 imaging.<sup>243</sup> Several factors, including size, shape, and surface coating, influence the sensitivity of manganese oxide NPs to T1 contrast-enhanced MRI.<sup>244</sup> Hyeon et al have synthesized MnO NPs of varying sizes and observed that as the size decreases, the T1 relaxation time is shortened, leading to enhanced signal intensity. This effect is attributed to the increased surface area of the smaller NPs, which facilitates enhanced interaction with water molecules.<sup>245</sup> Supporting this notion, Yang et al have demonstrated that increasing the surface area of MnO NPs through size and shape design results in favorable enhancement in T1 imaging of hepatic tumors.<sup>246</sup> To enhance the diagnostic capabilities of MRI, surface-functionalized and/or stimulation-responsive manganese oxide NPs have garnered considerable attention. For instance, Wei et al have developed small-sized octagonal hollow porous manganese oxide NPs functionalized with zwitterionic dopamine sulfonate as a pH-responsive MRI contrast agent for real-time monitoring of HCC. The r1 relaxivity value of the manganese oxide NPs is only 0.8 mM<sup>-1</sup> s<sup>-1</sup> at pH 7.4, but it increases to 5.2 mM<sup>-1</sup> s<sup>-1</sup> and 8.3 mM<sup>-1</sup> s<sup>-1</sup> in acidic solutions at pH 6.5 and 5.4, respectively. This pH-dependent enhancement enables precise imaging and diagnosis of HCC.<sup>247</sup> Thus, manganese oxide NPs offer a novel, safe, and accurate nanoplatform for future precise imaging and diagnosis of GI conditions.

In contrast to T1 contrast agents, IONPs serve as T2 contrast agents, providing negative contrast enhancement by shortening the T2 relaxation time of protons. This contrast mechanism can sometimes lead to challenges in distinguishing between normal tissue and lesions due to the low contrast presented by magnetic NPs.<sup>227</sup> However, IONPs still possess numerous appealing advantages, including high sensitivity, excellent compatibility, and biosafety.<sup>248</sup> Furthermore, the engineering and functionalization of IONPs have been employed to address these challenges.<sup>14,249</sup> For instance, Li et al have designed a novel contrast agent called glycyrrhetic acid (GA) group-modified Fe<sub>3</sub>O<sub>4</sub> NPs (Fe<sub>3</sub>O<sub>4</sub>@cGlu-GA) for liver tumor-targeted MRI. Fe<sub>3</sub>O<sub>4</sub>@cGlu-GA NPs exhibit excellent targeting capabilities towards HCC cells, along with good biocompatibility and ultra-low hepatotoxicity.<sup>182</sup> Nishimura et al have utilized ferumoxtran-10, an ultrasmall SPIONP, to evaluate the efficacy of MRI in diagnosing lymph node metastasis in esophageal cancer. The results demonstrate a sensitivity of 100%, specificity of 95.4%, and accuracy of 96.2% in differentiating benign from malignant lymph nodes in esophageal cancer.<sup>250</sup> Moreover, SPIONPs have proven valuable as cell labels or tracers for MRI. Wu et al have employed SPIONP-labeled macrophages in IBD for MRI assessment of disease activity. In vitro mass spectrometry confirms the high uptake capacity of macrophages for SPIONPs. MRI reveals approximately 3% of the injected dose of SPIONP-labeled macrophages present in the intestine within 24 hours of administration, indicating the potential of using MRI to monitor the inflammatory activity of IBD.<sup>16</sup>

NP-based activatable MRI contrast agents have gained significant attention in recent years due to their ability to switch between “off” and “on” states based on specific stimuli in the surrounding physiological environment, such as pH or enzymes.<sup>251,252</sup> These contrast agents offer the advantage of providing signal enhancement selectively in the target area, improving the sensitivity and specificity of MRI. For instance, Lee et al have designed magnetic IONPs that are targeted to the urokinase plasminogen activator receptor (uPAR) and loaded with the chemotherapy drug gemcitabine (Gem). These NPs are designed for targeted delivery to uPAR-expressing tumor cells. Upon internalization by the tumor cells via endocytosis, the NPs release Gem intracellularly, leading to enhanced MRI contrast, specifically in pancreatic cancer cells.<sup>253</sup> Similarly, Shi et al have reported the development of a tumor-targeted and enzyme-activated nanoprobe composed of a tumor-targeting ligand (cRGD) and a matrix metalloproteinase-2 (MMP-2)-cleavable fluorescent substrate-

modified gadolinium-doped CuS micellar NPs. This nanoprobe selectively accumulates in gastric tumors after intravenous injection in mice, and upon MMP activation, the MRI shows a significant increase in r1 relaxivity. The enzyme-activating nanoprobe demonstrates enhanced MRI of tumors, highlighting its potential as a promising tool for early diagnosis of gastric tumors.<sup>17</sup> These studies demonstrate the potential of activatable NP-based MRI contrast agents to improve the specificity and sensitivity of tumor imaging, enabling targeted delivery of therapeutic agents and early detection of tumors.

## US

US imaging is widely employed in clinical diagnostics due to its safety, non-invasiveness, non-ionizing nature, affordability, high spatial resolution, and real-time imaging capabilities.<sup>254</sup> This imaging modality utilizes ultrasound waves to scan the human body, capturing reflected signals that are subsequently received and processed to generate images of tissues and organs.<sup>255</sup> Conventional US contrast agents typically consist of microbubbles ranging from 1 to 8 microns in size, such as Levovist, SonoVue, and Optison. These agents provide only blood flow signal owing to their large particle size, shorter circulation time, and relatively lower stability.<sup>256</sup> In contrast, NP-based contrast agents, leveraging the EPR effect, exhibit the potential for accumulation at tumor sites, thereby showing promise for extravascular imaging in US.<sup>257</sup> Furthermore, the surfaces of NPs can be modified with functional groups (such as antibodies, peptides, folic acids, nucleic acids, etc.) to actively target specific tissues, thereby enhancing the contrast in US imaging.<sup>258–260</sup>

Currently, NP-based contrast agents can be classified into three main types: gas-based NPs, liquid-based NPs, and solid-based NPs. Gas-based NPs utilize cores, such as carbon dioxide (CO<sub>2</sub>), nitrogen, perfluorocarbon, and sulfur hexafluoride, with shells composed of liposomes, polymer NPs, or silica NPs.<sup>261–266</sup> Similarly, liquid-based NPs, like perfluorooctyl bromide NPs, possess a core-shell structure akin to gas-based NPs.<sup>267</sup> Moreover, solid-based NPs, such as silica NPs, which are smaller in size compared to gas-based NPs, generate strong US signals by aggregating at lesion sites through active or passive targeting mechanisms.<sup>268</sup> The utilization of NP-based enhanced US imaging holds great promise in the diagnosis of GI diseases.<sup>269</sup> For instance, Hu et al have successfully synthesized a targeted nanoprobe by incorporating a folate-PEG-chitosan derivative shell and a perfluorooctyl bromide nanocore. This nanoprobe demonstrates excellent biocompatibility and targeted capability, exhibiting specific accumulation in HCC cell lines to enhance US imaging.<sup>256</sup> Moreover, nanobubbles have shown potential for extravascular US imaging owing to their high penetration power and stability. Fan et al have developed nanobubbles with a particle size of  $435.2 \pm 60.53$  nm and evaluated their contrast effect in a gastric cancer xenograft model. These nanobubbles exhibit enhanced US imaging compared to SonoVue microbubbles, penetrating the tissue space of gastric cancer and providing morphological evidence of tumor angiogenesis.<sup>185</sup>

Furthermore, combining US imaging with other imaging techniques can offer compelling evidence for the early diagnosis of GI diseases. For example, Maghsoudinia et al have developed folic acid-targeted phase-change nanodroplets loaded with gadolinium, enabling dual-modal MRI/US imaging of HCC. This dual-functional contrast agent not only enhances the US signal but also exhibits a high r1 relaxivity, providing improved diagnostic capabilities.<sup>270</sup> Additionally, the use of activatable nanoprobe allows for the integration of therapeutic and US imaging functionalities, opening new possibilities for diagnosis and treatment.<sup>271,272</sup> Go et al have demonstrated the potential of ketonized maltodextrin NPs as both US contrast agents and drug delivery carriers in mouse models of acute liver failure. The NPs undergo hydrolytic degradation triggered by acid, resulting in the generation of CO<sub>2</sub> bubbles that enhance the US signal while facilitating drug release.<sup>273</sup> Similarly, Chen et al have successfully developed a targeted US contrast agent composed of gas-generating calcium carbonate/pullulan-graft-poly(carboxybetaine methacrylate) hybrid NPs, which are targeted by pullulan, for liver cancer diagnosis. The nanocomplex exhibits excellent vascular permeability and stability. Under the acidic pH conditions of the tumor, the calcium carbonate NPs decompose, generating CO<sub>2</sub> and significantly enhancing the US contrast at the tumor site while leaving normal tissue unaffected.<sup>272</sup>

Although NPs have initially shown promise in improving the accuracy of US imaging for the diagnosis of GI diseases, it is evident that their potential in this area has not been thoroughly explored, as evidenced by the limited number of reported studies. It is anticipated that the development of novel NP-based US contrast agents with longer half-

lives, higher stability, and enhanced specificity for specific cells and tissues will further enhance the sensitivity and specificity of US imaging in the diagnosis of digestive diseases, thereby expanding its applications.

## PET

PET is an imaging technology that utilizes short-lived positron-emitting radionuclides, such as carbon ( $^{11}\text{C}$ ), nitrogen ( $^{15}\text{N}$ ), oxygen ( $^{15}\text{O}$ ), or fluorine ( $^{18}\text{F}$ ) to label compounds involved in cellular metabolism, enabling the measurement of metabolic activity for diagnostic purposes.<sup>274–276</sup> Despite limitations, such as high clinical cost and radioactive exposure, PET plays a crucial role in the diagnosis of soft tissues due to its high tissue penetration, sensitivity, specificity, and real-time dynamic imaging capabilities.<sup>277</sup> In comparison to MRI and CT, PET can facilitate early diagnosis even before the morphological changes in the lesion area become apparent, and it can differentiate between benign and malignant tumors based on the high metabolic activity of malignant tumors.<sup>277,278</sup> PET is highly effective in tumor staging and the detection of micrometastases.<sup>279</sup> Additionally, PET demonstrates superior diagnostic capabilities for inflammatory diseases like IBD due to increased glycolytic activity in these conditions.<sup>280</sup>

The main contrast agent used in clinical practice for PET is 18-fluorine-fluorodeoxyglucose ( $^{18}\text{F}$ -FDG). However, a significant clinical challenge lies in the potential for false-positive results introduced by these radiopharmaceuticals. Therefore, the development of NP-based PET contrast agents is crucial to overcome this challenge. Several studies have already demonstrated the potential of NP-based PET in the diagnosis of GI diseases. Liposomal radiotracers have emerged as promising nuclear imaging probes, and various methods for radionuclide labeling (such as encapsulation within liposomes to protect them from enzymatic degradation or protein binding) and synthetic strategies, have been extensively investigated to enhance their biocompatibility, stability, and specific targeting capabilities.<sup>281</sup> For example, Lee et al have introduced a novel PET imaging strategy that capitalizes on the differential esterase activity of tumors and mononuclear phagocyte system organs. They utilize  $^{124}\text{I}$ -labeled liposomes as radiotracers, which are rapidly eliminated from the liver and spleen upon cleavage by esterases. In contrast, the lipophilic radiotracer delivered to the tumor is retained, resulting in enhanced SNR between tumors and surrounding tissues/organs. This approach proves valuable for the early diagnosis of pancreatic cancer, offering improved imaging sensitivity and specificity.<sup>18</sup> Dendrimers have also shown promise as multifunctional scaffolds for the development of PET imaging agents due to their unique characteristics. Garrigue et al have developed a  $^{68}\text{Ga}$  radiolabeled amphiphilic dendrimer for PET imaging, employing EPR-mediated passive tumor targeting in various xenograft mouse models, including CRC and pancreatic adenocarcinoma. The nanosystem exhibits excellent imaging sensitivity and specificity, demonstrating a 14-fold increase in PET signal ratio compared to  $^{18}\text{F}$ -FDG.<sup>282</sup> Moreover, micelles have emerged as effective delivery vehicles for PET imaging agents, offering prolonged circulation time, specific tumor uptake, and stimulus responsiveness.<sup>283</sup> For example, pH-sensitive  $^{64}\text{Cu}$ -labeled neutral copolymer micelles undergo breakdown in the acidic tumor environment, resulting in the formation of polycationic polymers that are selectively retained by cancer cells. PET imaging utilizing  $^{64}\text{Cu}$ -labeled polymer micelles demonstrates superior contrast for the detection of small occult tumors compared to  $^{18}\text{F}$ -FDG.<sup>284</sup>

Targeted molecular PET imaging has emerged as a powerful approach for obtaining high-quality images through the specific binding of ligands and active accumulation of radiotracers at the site of GI tumors. Girgis et al have investigated the efficacy of  $^{124}\text{I}$ -labeled anti-CA19-9 cys-diabody in combination with polymeric liposome NPs for PET imaging of pancreatic cancer. This approach achieves specific molecular imaging with a tumor-to-blood ratio of 3, demonstrating its effectiveness.<sup>19</sup> In another study, Zhang et al have designed  $^{64}\text{Cu}$ -labeled ultrasmall copper NPs targeted to CC chemokine receptor 2 for PET imaging of pancreatic ductal adenocarcinoma in a mouse model. These targeted NPs exhibit high sensitivity and effectiveness in detecting the disease.<sup>20</sup> Similarly, Paiva et al have developed  $^{64}\text{Cu}$ -labeled GE11-modified polymeric micellar NPs for PET imaging in a CRC model. By targeting the EGFR, the GE11-modified micelles show increased accumulation in colon cancer cells compared to untargeted micelles, thereby enhancing the contrast of PET imaging.<sup>21</sup> Also, targeted molecular PET imaging is suitable for the diagnosis and differential diagnosis of IBD and the assessment of inflammation. Dearling et al have prepared  $^{64}\text{Cu}$ -labeled anti-beta (7) integrin antibody (FIB504.64) for PET radioimmunoassay in colitis. The study demonstrates that  $^{64}\text{Cu}$ -labeled anti- $\beta$  (7) integrin antibodies are selectively absorbed in the intestines of colitis animals and exhibit higher uptake compared to the controls, thereby enhancing PET imaging of IBD.<sup>285</sup> Furthermore, Freise et al have developed a PET probe for the detection of  $\text{CD4}^+$  T cells in an IBD mouse

model. They use  $^{89}\text{Zr}$ -labeled CD4 antibody fragment (GK1.5 cDb) to efficiently recognize  $\text{CD4}^+$  T cells in the colon, cecum, and mesenteric lymph nodes of mice with colitis, thereby demonstrating increased inflammatory activity in these specific sites.<sup>280</sup>

To enhance the accuracy of imaging, the combination of NP-based PET imaging with other imaging techniques, such as MRI, CT, and fluorescence, is being explored for the diagnosis of GI diseases. Kim et al have designed a novel dual-modality tumor-targeted agent by labeling oleanolic acid-conjugated IONPs with  $^{68}\text{Ga}$  for PET/MRI in CRC mouse models. This targeted agent exhibits high uptake by CRC cells, enabling effective PET/MRI imaging.<sup>286</sup> Therefore, NP-based PET/MRI imaging holds great promise in the diagnosis of digestive diseases. However, there are still hurdles that need to be addressed, including the conjugation of radiopharmaceuticals to NPs, precise delivery and release of NPs, and other crucial considerations, such as appropriate isotopes, effective radiolabeling strategies, specific targeting modifications, and favorable pharmacokinetic profiles. These aspects require further in-depth research and investigation.

## Limitations and Prospects

NPs utilized in biomedical imaging offer several attractive advantages. Their small sizes and modifiable surfaces enable them to evade phagocytosis by the reticuloendothelial system (RES) and to selectively accumulate at desired sites through the EPR effect or active targeting. Furthermore, the high surface-to-volume ratio of NPs enhances their capacity to carry contrast agents and drugs while also improving their stability and safety. Currently, various types of NPs with unique properties are successfully employed in imaging technologies. IONPs possess superparamagnetic properties that make them highly suitable for MRI. AuNPs are widely used in CT imaging due to their high X-ray attenuation coefficient and versatile surface chemistry. QDs, with their tunable sizes, exhibit promising fluorescent properties and can emit visible fluorescence at different wavelengths, making them valuable in fluorescence imaging. Moreover, UCNPs, capable of converting multiple low-energy photons into high-energy photons, are actively being explored as emerging players in optical imaging technologies. Additionally, fluorescent probes combined with exosomes can be employed to specifically identify tumors. Engineered exosomes with targeted modifications enable the targeted delivery of fluorescent tracers for the specific diagnosis of diseases.<sup>287–290</sup> This detection method has shown successful development, as illustrated in [Figure 3](#). Consequently, the future utilization of NP-based imaging technologies holds great promise for the diagnosis of GI diseases.

While the results of research on NPs in modern imaging techniques are exciting, they remain insufficient for their true translation into clinically practical imaging agents. When utilizing NPs as contrast agents for medical imaging, it is crucial to consider their *in vivo* toxicity. Extensive *in vivo* and *in vitro* studies have demonstrated that many NPs pose varying degrees of toxicity risk. As foreign materials, NPs interact with biological systems and can induce adverse effects through physical, chemical, and immunological mechanisms, including oxidative stress, genotoxicity, immunogenicity, apoptosis, and necrosis.<sup>8,292</sup> Furthermore, aside from the inherent toxicity of certain NPs, such as cadmium in QDs, excessive retention or impaired clearance of NPs in the body can lead to nanotoxicity, resulting in issues like capillary occlusion, aggregation leading to functional loss and damage to organs such as the liver, spleen, lung, and kidneys. Although adjusting the size, shape, composition, surface chemistry, and other factors of NPs can reduce the toxicity risk, as seen with silica-coated QDs, achieving true translation into clinical diagnostic applications remains an extremely challenging task. For instance, if NPs are not efficiently eliminated from the body following injection, a significant amount of time is required to assess the effects of the administered dose and the long-term toxicity implications on the body. Secondly, it is crucial to address the delivery challenges associated with NPs targeting the GI tract. When administered intravenously, NPs face multiple biological barriers *in vivo* that hinder their delivery to the GI ailment site. Phagocytosis by the monocyte-phagocyte system (spleen and liver) results in the nonspecific distribution of NPs in healthy organs, leading to inadequate accumulation at the desired disease locations. Moreover, blood rheology and intra-tumor hypertension present significant obstacles to NP delivery.<sup>293</sup> Compared to intravenous injection, oral administration offers certain advantages for the GI tract, including convenience, excellent safety, and positive patient acceptability. However, the complex environment of the GI tract, characterized by factors such as intestinal pH, diverse enzymes, intestinal microbiota, and the mucus barrier, continues to pose challenges to the effective absorption of NP formulations.<sup>9</sup> Therefore, to effectively overcome these barriers to NP delivery, a re-conceptualization of conventional NPs is required, taking into account factors such as size, shape, surface modification, and other relevant parameters. Similarly, the



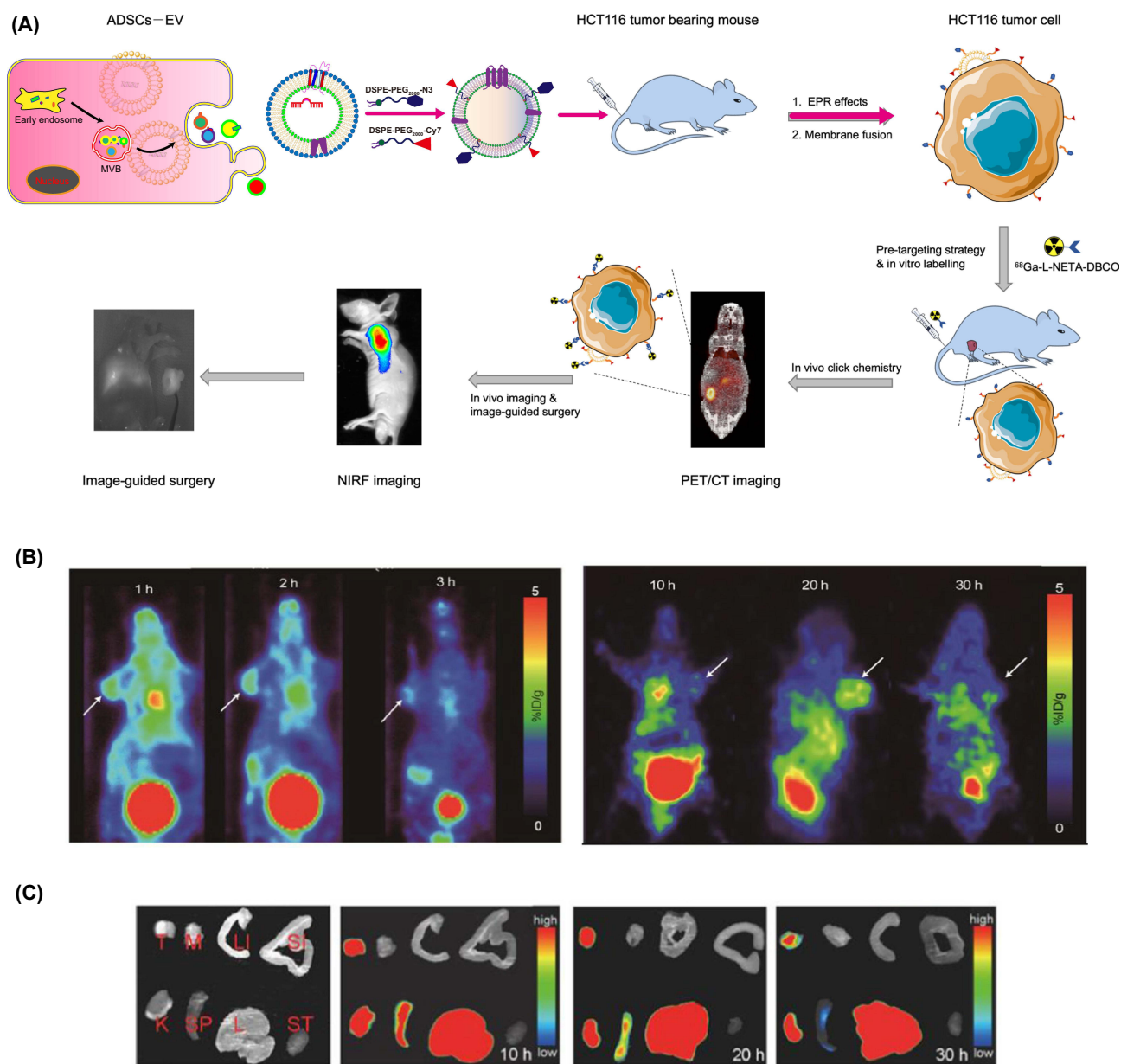


**Figure 3** Multimodal PET and NIRF imaging based on ADSCs derived extracellular vesicles. **(A)** Schematic illustration showing the generation of exosome use for bio-imaging. **(B)** NIRF imaging of gastrointestinal tumor-bearing nude mice at different time points (1, 5, 10, 20, 30 and 50 h). The arrows indicate tumor sites. **(C)** In vitro tissue images at different time points (10, 20 and 30 h) after injection of Cy7-EV-N3.

**Abbreviations:** M, muscle, LI, large intestine, SI, small intestine, K, kidney, SP, spleen, L, liver, ST, stomach.<sup>291</sup>

biocompatibility of NPs and their degradation products in vivo must be taken into consideration for practical diagnostic applications. Organic NPs generally exhibit better biocompatibility compared to heavy metals, highlighting the importance of developing synthesis strategies that prioritize biocompatible and biodegradable NPs. Besides, the targeting mechanism of NPs improves the efficiency of imaging agents in reaching their intended targets while minimizing side effects associated with nonspecific accumulation in the organism. However, NPs or nanocarriers in vivo are susceptible to enzymatic degradation and phagocytosis by RES. Thus, in the complex physiological environment of the body, achieving precise targeting of the desired site without significant accumulation in other areas remains a significant challenge. It is crucial to enhance the stability of NP-ligand interactions, improve the affinity between ligands and receptors, and mitigate the toxic side effects that may arise from the off-target accumulation of contrast agents. Furthermore, limitations such as inadequate availability of certain raw materials, high synthesis costs, and the use of

toxic solvents during the synthesis process can impede the clinical translation of NPs. Therefore, it is imperative to explore the use of non-toxic, environmentally friendly, and abundant natural resources in the development of NPs. Overcoming these challenges is crucial to unlock the vast potential of NP-based imaging technologies in the diagnosis of GI diseases in the near future.

Currently, the majority of studies in the field have been conducted in animal models, with only a limited number of studies applying NP-based imaging techniques in clinical practice. Therefore, it is crucial to accelerate the pace of the clinical translation of NPs. In this regard, we presented several exciting directions for future applications of NPs in GI disease imaging combined with clinical practice. Firstly, considering the variations in patient conditions and disease characteristics, a single imaging approach often falls short of providing comprehensive information about a patient's disease. To overcome this limitation, the development of versatile NP-based multimodal imaging strategies is essential. By combining multiple imaging modalities, these approaches can achieve high sensitivity and specificity in diagnosis. Future efforts should focus on designing multifunctional NPs that not only optimize the combination and ratio of various imaging agents but also enable the selection of imaging modes that synergistically enhance diagnostic capabilities. Secondly, targeted molecular imaging represents a significant advancement in current research. The incorporation of multiple targeting ligands onto NPs can greatly enhance binding affinity and specificity, facilitating the effective accumulation of imaging agents at the site of interest. This enables precise identification of lesions, particularly in early-stage tumors, without adversely affecting other organs and tissues. Moreover, the use of specific stimuli, such as pH, enzymes, and light, can serve as “switches” to activate NPs at the targeted sites, enhancing their imaging performance. Hence, targeted molecular imaging is a worthy direction for future exploration, with a focus on the selection of appropriate ligands for NPs and ensuring their stability *in vivo*. Furthermore, in order to overcome the delivery barriers associated with GI-targeting NPs, several stealth NP strategies have been developed, including the use of PEG-functionalized NPs, which effectively evade clearance by the monocyte-phagocyte system.<sup>294</sup> Another approach is the “cluster bomb” oral drug delivery method, employing a pH-sensitive core-shell structure to precisely control drug release in the intestinal microenvironment. This approach also utilizes an LV-modified surface to overcome the epithelial barrier and enhance drug accumulation at the tumor site.<sup>295</sup> Furthermore, NP hitchhiking designs have demonstrated the ability to overcome biological barriers and actively aggregate at disease sites, involving erythrocytes, neutrophils, macrophages, and probiotics.<sup>296–298</sup> Therefore, these NP strategies for addressing delivery barriers represent a crucial area of future research. Finally, the significance of endoscopy in the diagnosis of GI diseases is self-evident. By harnessing the unique physicochemical properties of NPs, such as fluorescence, it becomes possible to visualize structural and morphological changes in GI diseases, enabling early identification of lesions, particularly in cases of early-stage cancers. Consequently, NP-based endoscopy optical imaging is a direction deserving our intensive research in the future. NPs are not silver bullets but rather assistive tools that need to be carefully tailored and selected to align with specific imaging technologies, ensuring their optimal performance in diagnostics.

## Conclusion

Taken together, NP-based imaging technologies provide a promising diagnostic strategy for GI diseases. These technologies not only provide more comprehensive disease information by integrating multiple imaging contrast agents into a single nanoprobe but also enhance the specificity and sensitivity of imaging through the effective accumulation of nanoprobes carrying multiple targeting ligands at the site of the lesion. Despite their attractiveness, there are still certain challenges that need to be addressed for the clinical translation of NP-based imaging techniques. These include ensuring the safety of NPs, achieving specific targeting, and improving cost-effectiveness. It is our hope that the advantages of NPs in imaging technologies can be maximized while minimizing their disadvantages, thereby advancing the field of gastroenterology diagnostics and making significant contributions to human health in the near future.

## Abbreviations

GI, gastrointestinal; IBD, inflammatory bowel disease; UC, ulcerative colitis; CD, Crohn's disease; CRC, colorectal cancer; US, ultrasonography; CT, computed tomography; MRI, magnetic resonance imaging; PET, positron emission tomography; NP, nanoparticle; EPR, enhanced permeability and retention; NWs, nanowires; SERS, surface-enhanced

Raman scattering; SNR, signal-to-noise ratio; IONPs, iron oxide nanoparticles; EGFR, epithelial growth factor receptor; SPIONPs, superparamagnetic iron oxide nanoparticles; QDs, quantum dots; HCC, hepatocellular carcinoma; NIR, near-infrared; NIRF, near-infrared fluorescence; CNTs, carbon nanotubes; SWCNTs, single-walled carbon nanotubes; MWCNTs, multi-walled carbon nanotubes; AuNPs, gold nanoparticles; PECNPs, polyelectrolyte complex nanoparticles; UCNPs, upconversion nanoparticles; CaPNPs, calcium phosphate nanoparticles; PFCNPs, perfluorocarbon nanoparticles; UCL, upconversion luminescence; SPECT, single photon emission computed tomography; WLE, white light endoscopy; Gd-DTPA, gadolinium-diethylenetriaminepentaacetic acid; SLNs, solid-lipid nanoparticles; MMP-2, matrix metalloproteinase-2; <sup>18</sup>F-FDG, 18-fluorine-fluorodeoxyglucose; RES, reticuloendothelial system.

## Acknowledgment

We thank funding from Science and Technology Innovation Committee of Shenzhen (No. JCYJ20150403101028164, No. JCYC20170307100911479, No. JCYJ20190807145617113 and JCYJ20210324113802006), the Technical Research and Development Project of Shenzhen (No. JCYJ2022053015180024), the Shenzhen Fund for Guangdong Provincial High Level Clinical Key Specialties (Grant SZGSP013), and the Shenzhen Key Medical Discipline Construction Fund (Grant SZXK042).

## Disclosure

The authors declare no conflicts of interest in this work.

## References

1. Sung H, Ferlay J, Siegel RL, et al. Global Cancer Statistics 2020: GLOBOCAN Estimates of Incidence and Mortality Worldwide for 36 Cancers in 185 Countries. *CA Cancer J Clin.* 2021;71(3):209–249. doi:10.3322/caac.21660
2. Ng SC, Shi HY, Hamidi N, et al. Worldwide incidence and prevalence of inflammatory bowel disease in the 21st century: a systematic review of population-based studies. *Lancet Lond Engl.* 2017;390(10114):2769–2778. doi:10.1016/S0140-6736(17)32448-0
3. Tian CM, Zhang Y, Yang MF, et al. Stem cell therapy in inflammatory bowel disease: a review of achievements and challenges. *J Inflamm Res.* 2023;16:2089–2119. doi:10.2147/JIR.S400447
4. Tian CM, Yang MF, Xu HM, et al. Mesenchymal stem cell-derived exosomes: novel therapeutic approach for inflammatory bowel diseases. *Stem Cells Int.* 2023;2023:4245704. doi:10.1155/2023/4245704
5. Mezoff EA, Williams KC, Erdman SH. Gastrointestinal endoscopy in the neonate. *Clin Perinatol.* 2020;47(2):413–422. doi:10.1016/j.clp.2020.02.012
6. Dassen AE, Lips DJ, Hoekstra CJ, Puijdt JFM, Bosscha K. FDG-PET has no definite role in preoperative imaging in gastric cancer. *Eur J Surg Oncol J Eur Soc Surg Oncol Br Assoc Surg Oncol.* 2009;35(5):449–455. doi:10.1016/j.ejso.2008.11.010
7. Mitchell MJ, Billingsley MM, Haley RM, Wechsler ME, Peppas NA, Langer R. Engineering precision nanoparticles for drug delivery. *Nat Rev Drug Discov.* 2021;20(2):101–124. doi:10.1038/s41573-020-0090-8
8. Chen G, Roy I, Yang C, Prasad PN. Nanochemistry and Nanomedicine for Nanoparticle-based Diagnostics and Therapy. *Chem Rev.* 2016;116(5):2826–2885. doi:10.1021/acs.chemrev.5b00148
9. Li DF, Yang MF, Xu HM, et al. Nanoparticles for oral delivery: targeted therapy for inflammatory bowel disease. *J Mater Chem B.* 2022;10(31):5853–5872. doi:10.1039/d2tb01190e
10. Khan FA, Albalawi R, Pottoo FH. Trends in targeted delivery of nanomaterials in colon cancer diagnosis and treatment. *Med Res Rev.* 2022;42(1):227–258. doi:10.1002/med.21809
11. Wu Y, Briley K, Tao X. Nanoparticle-based imaging of inflammatory bowel disease. *Wiley Interdiscip Rev Nanomed Nanobiotechnol.* 2016;8(2):300–315. doi:10.1002/wnan.1357
12. Zhou J, Chen L, Chen L, Zhang Y, Yuan Y. Emerging role of nanoparticles in the diagnostic imaging of gastrointestinal cancer. *Semin Cancer Biol.* 2022. doi:10.1016/j.semcancer.2022.04.009
13. Xing X, Zhang B, Wang X, Liu F, Shi D, Cheng Y. An “imaging-biopsy” strategy for colorectal tumor reconfirmation by multipurpose paramagnetic quantum dots. *Biomaterials.* 2015;48:16–25. doi:10.1016/j.biomaterials.2015.01.011
14. Tanimoto A, Kuribayashi S. Application of superparamagnetic iron oxide to imaging of hepatocellular carcinoma. *Eur J Radiol.* 2006;58(2):200–216. doi:10.1016/j.ejrad.2005.11.040
15. Wang P, Qu Y, Li C, et al. Bio-functionalized dense-silica nanoparticles for MR/NIRF imaging of CD146 in gastric cancer. *Int J Nanomedicine.* 2015;10:749–763. doi:10.2147/IJN.S62837
16. Wu Y, Briley-Saebo K, Xie J, et al. Inflammatory bowel disease: MR- and SPECT/CT-based macrophage imaging for monitoring and evaluating disease activity in experimental mouse model—pilot study. *Radiology.* 2014;271(2):400–407. doi:10.1148/radiol.13122254
17. Shi H, Sun Y, Yan R, et al. Magnetic Semiconductor Gd-Doping CuS Nanoparticles as Activatable Nanoprobes for Bimodal Imaging and Targeted Photothermal Therapy of Gastric Tumors. *Nano Lett.* 2019;19(2):937–947. doi:10.1021/acs.nanolett.8b04179
18. Lee W, Il An G, Park H, et al. Imaging Strategy that Achieves Ultrahigh Contrast by Utilizing Differential Esterase Activity in Organs: application in Early Detection of Pancreatic Cancer. *ACS Nano.* 2021;15(11):17348–17360. doi:10.1021/acsnano.1c05165
19. Girgis MD, Federman N, Rochefort MM, et al. An engineered anti-CA19-9 cys-diabody for positron emission tomography imaging of pancreatic cancer and targeting of polymerized liposomal nanoparticles. *J Surg Res.* 2013;185(1):45–55. doi:10.1016/j.jss.2013.05.095

20. Zhang X, Detering L, Sultan D, et al. Chemokine Receptor 2-Targeting Copper Nanoparticles for Positron Emission Tomography-Guided Delivery of Gemcitabine for Pancreatic Ductal Adenocarcinoma. *ACS Nano*. 2021;15(1):1186–1198. doi:10.1021/acsnano.0c08185
21. Paiva I, Mattingly S, Wuest M, et al. Synthesis and Analysis of <sup>64</sup>Cu-Labeled GE11-Modified Polymeric Micellar Nanoparticles for EGFR-Targeted Molecular Imaging in a Colorectal Cancer Model. *Mol Pharm*. 2020;17(5):1470–1481. doi:10.1021/acs.molpharmaceut.9b01043
22. Wang S, Li W, Yuan D, Song J, Fang J. Quantitative detection of the tumor-associated antigen large external antigen in colorectal cancer tissues and cells using quantum dot probe. *Int J Nanomedicine*. 2016;11:235–247. doi:10.2147/IJN.S97509
23. Wang YW, Kang S, Khan A, Bao PQ, Liu JTC. In vivo multiplexed molecular imaging of esophageal cancer via spectral endoscopy of topically applied SERS nanoparticles. *Biomed Opt Express*. 2015;6(10):3714–3723. doi:10.1364/BOE.6.003714
24. Dassie E, Arcidiacono D, Wasiak I, et al. Detection of fluorescent organic nanoparticles by confocal laser endomicroscopy in a rat model of Barrett's esophageal adenocarcinoma. *Int J Nanomedicine*. 2015;10:6811–6823. doi:10.2147/IJN.S86640
25. Cheng CC, Huang CF, Ho AS, et al. Novel targeted nuclear imaging agent for gastric cancer diagnosis: glucose-regulated protein 78 binding peptide-guided <sup>111</sup>In-labeled polymeric micelles. *Int J Nanomedicine*. 2013;8:1385–1391. doi:10.2147/IJN.S42003
26. Wang K, Ruan J, Qian Q, et al. BRCA1 monoclonal antibody conjugated fluorescent magnetic nanoparticles for in vivo targeted magneto-fluorescent imaging of gastric cancer. *J Nanobiotechnology*. 2011;9:23. doi:10.1186/1477-3155-9-23
27. Chee HL, Gan CRR, Ng M, et al. Biocompatible Peptide-Coated Ultrasmall Superparamagnetic Iron Oxide Nanoparticles for In Vivo Contrast-Enhanced Magnetic Resonance Imaging. *ACS Nano*. 2018;12(7):6480–6491. doi:10.1021/acsnano.7b07572
28. Li X, Liu L, Fu Y, et al. Peptide-enhanced tumor accumulation of upconversion nanoparticles for sensitive upconversion luminescence/magnetic resonance dual-mode bioimaging of colorectal tumors. *Acta Biomater*. 2020;104:167–175. doi:10.1016/j.actbio.2020.01.003
29. Lambidis E, Chen CC, Lumen D, et al. Biological evaluation of integrin  $\alpha 3 \beta 1$ -targeted 68Ga-labeled HEVNs in HCT 116 colorectal tumor-bearing mice. *Eur J Pharm Sci off J Eur Fed Pharm Sci*. 2023;180:106336. doi:10.1016/j.ejps.2022.106336
30. Xiang Y, Yang H, Guo X, et al. Surface enhanced Raman detection of the colon cancer biomarker cytidine by using magnetized nanoparticles of the type Fe<sub>3</sub>O<sub>4</sub>/Au/Ag. *Mikrochim Acta*. 2018;185(3):195. doi:10.1007/s00604-017-2666-5
31. Du Y, Fan K, Zhang H, et al. Endoscopic molecular imaging of early gastric cancer using fluorescently labeled human H-ferritin nanoparticle. *Nanomed Nanotechnol Biol Med*. 2018;14(7):2259–2270. doi:10.1016/j.nano.2018.07.007
32. Qiao R, Liu C, Liu M, et al. Ultrasensitive in vivo detection of primary gastric tumor and lymphatic metastasis using upconversion nanoparticles. *ACS Nano*. 2015;9(2):2120–2129. doi:10.1021/nn507433p
33. Li Y, Hu X, Ding D, et al. In situ targeted MRI detection of Helicobacter pylori with stable magnetic graphitic nanocapsules. *Nat Commun*. 2017;8:15653. doi:10.1038/ncomms15653
34. Bartoş A, Bartoş D, Szabo B, et al. Recent achievements in colorectal cancer diagnostic and therapy by the use of nanoparticles. *Drug Metab Rev*. 2016;48(1):27–46. doi:10.3109/03602532.2015.1130052
35. Doucey MA, Carrara S. Nanowire Sensors in Cancer. *Trends Biotechnol*. 2019;37(1):86–99. doi:10.1016/j.tibtech.2018.07.014
36. Araki T, Uemura T, Yoshimoto S, et al. Wireless Monitoring Using a Stretchable and Transparent Sensor Sheet Containing Metal Nanowires. *Adv Mater Deerfield Beach Fla*. 2020;32(15):e1902684. doi:10.1002/adma.201902684
37. Bu C, Mu L, Cao X, Chen M, She G, Shi W. Silver Nanowire-Based Fluorescence Thermometer for a Single Cell. *ACS Appl Mater Interfaces*. 2018;10(39):33416–33422. doi:10.1021/acsnano.8b09696
38. Zhang A, Lieber CM. Nano-Bioelectronics. *Chem Rev*. 2016;116(1):215–257. doi:10.1021/acs.chemrev.5b00608
39. Dasgupta NP, Sun J, Liu C, et al. 25th anniversary article: semiconductor nanowires--synthesis, characterization, and applications. *Adv Mater Deerfield Beach Fla*. 2014;26(14):2137–2184. doi:10.1002/adma.201305929
40. Milano G, D'Ortenzi L, Bejtka K, et al. Metal-insulator transition in single crystalline ZnO nanowires. *Nanotechnology*. 2021;32(18):185202. doi:10.1088/1361-6528/abe072
41. Bayrak T, Jagtap NS, Erbe A. Review of the Electrical Characterization of Metallic Nanowires on DNA Templates. *Int J Mol Sci*. 2018;19(10):E3019. doi:10.3390/ijms19103019
42. Geng H, Chen X, Sun L, et al. ZnCuInSe/Au/TiO<sub>2</sub> sandwich nanowires-based photoelectrochemical biosensor for ultrasensitive detection of kanamycin. *Anal Chim Acta*. 2021;1146:166–173. doi:10.1016/j.aca.2020.11.017
43. Li KC, Chu HC, Lin Y, Tuan HY, Hu YC. PEGylated Copper Nanowires as a Novel Photothermal Therapy Agent. *ACS Appl Mater Interfaces*. 2016;8(19):12082–12090. doi:10.1021/acsnano.6b04579
44. Jo HS, Kwon HJ, Kim TG, et al. Wearable transparent thermal sensors and heaters based on metal-plated fibers and nanowires. *Nanoscale*. 2018;10(42):19825–19834. doi:10.1039/c8nr04810j
45. Gu L, Cao X, Mukhtar A, Wu K. Fe/Mn multilayer nanowires as dual mode  $\tau_1 - \tau_2$  magnetic resonance imaging contrast agents. *J Biomed Mater Res B Appl Biomater*. 2021;109(4):477–485. doi:10.1002/jbm.b.34715
46. Abbaspour M, Namayandeh jorabchi M, Akbarzadeh H, Salemi S, Ebrahimi R. Molecular dynamics simulation of anticancer drug delivery from carbon nanotube using metal nanowires. *J Comput Chem*. 2019;40(25):2179–2190. doi:10.1002/jcc.25867
47. Das B, Dadhich P, Pal P, Thakur S, Neogi S, Dhara S. Carbon nano dot decorated copper nanowires for SERS-Fluorescence dual-mode imaging/anti-microbial activity and enhanced angiogenic activity. *Spectrochim Acta A Mol Biomol Spectrosc*. 2020;227:117669. doi:10.1016/j.saa.2019.117669
48. Martínez-Banderas AI, Aires A, Plaza-García S, et al. Magnetic core-shell nanowires as MRI contrast agents for cell tracking. *J Nanobiotechnology*. 2020;18(1):42. doi:10.1186/s12951-020-00597-3
49. Ivanov YD, Romanova TS, Malsagova KA, Pleshakova TO, Archakov AI. Use of silicon nanowire sensors for early cancer diagnosis. *Mol Basel Switz*. 2021;26(12):3734. doi:10.3390/molecules26123734
50. Zheng G, Patolsky F, Cui Y, Wang WU, Lieber CM. Multiplexed electrical detection of cancer markers with nanowire sensor arrays. *Nat Biotechnol*. 2005;23(10):1294–1301. doi:10.1038/nbt1138
51. Nami M, Han P, Hanlon D, et al. Rapid Screen for Antiviral T-Cell Immunity with Nanowire Electrochemical Biosensors. *Adv Mater Deerfield Beach Fla*. 2022;34(29):e2109661. doi:10.1002/adma.202109661
52. Avasthi A, Caro C, Pozo-Torres E, Leal MP, García-Martín ML. Magnetic Nanoparticles as MRI Contrast Agents. *Top Curr Chem Cham*. 2020;378(3):40. doi:10.1007/s41061-020-00302-w

53. Zhou Z, Lu ZR. Gadolinium-based contrast agents for magnetic resonance cancer imaging: gadolinium-based CA for MR cancer imaging. *Wiley Interdiscip Rev Nanomed Nanobiotechnol.* 2013;5(1):1–18. doi:10.1002/wnan.1198
54. Ding N, Sano K, Kanazaki K, et al. In Vivo HER2-Targeted Magnetic Resonance Tumor Imaging Using Iron Oxide Nanoparticles Conjugated with Anti-HER2 Fragment Antibody. *Mol Imaging Biol.* 2016;18(6):870–876. doi:10.1007/s11307-016-0977-2
55. Chen L, Xie J, Wu H, et al. Improving sensitivity of magnetic resonance imaging by using a dual-targeted magnetic iron oxide nanoprobe. *Colloids Surf B Biointerfaces.* 2018;161:339–346. doi:10.1016/j.colsurfb.2017.10.059
56. Wang G, Qian K, Mei X. A theranostic nanoplatform: magneto-gold@fluorescence polymer nanoparticles for tumor targeting T 1 & T 2 -MRI /CT/NIR fluorescence imaging and induction of genuine autophagy mediated chemotherapy. *Nanoscale.* 2018;10(22):10467–10478. doi:10.1039/C8NR02429D
57. Zhang J, Ning Y, Zhu H, et al. Fast detection of liver fibrosis with collagen-binding single-nanometer iron oxide nanoparticles via T1-weighted MRI. *Proc Natl Acad Sci U S A.* 2023;120(18):e2220036120. doi:10.1073/pnas.2220036120
58. Bull E, Madani SY, Sheth R, Seifalian A, Green M, Seifalian AM. Stem cell tracking using iron oxide nanoparticles. *Int J Nanomedicine.* 2014;9:1641–1653. doi:10.2147/IJN.S48979
59. Yang L, Fu S, Liu L, et al. Tetraphenylethylene-conjugated polycation covered iron oxide nanoparticles for magnetic resonance/optical dual-mode imaging. *Regen Biomater.* 2021;8(3):rbab023. doi:10.1093/rb/rbab023
60. Adumeau P, Carnazza KE, Brand C, et al. A Pretargeted Approach for the Multimodal PET/NIRF Imaging of Colorectal Cancer. *Theranostics.* 2016;6(12):2267–2277. doi:10.7150/thno.16744
61. Deng S, Gu J, Jiang Z, et al. Application of nanotechnology in the early diagnosis and comprehensive treatment of gastrointestinal cancer. *J Nanobiotechnology.* 2022;20:415. doi:10.1186/s12951-022-01613-4
62. Mattoussi H, Palui G, Na HB. Luminescent quantum dots as platforms for probing in vitro and in vivo biological processes. *Adv Drug Deliv Rev.* 2012;64(2):138–166. doi:10.1016/j.addr.2011.09.011
63. Sarwat S, Stapleton F, Willcox M, Roy M. Quantum Dots in Ophthalmology: a Literature Review. *Curr Eye Res.* 2019;44(10):1037–1046. doi:10.1080/02713683.2019.1660793
64. Kargoza S, Hoseini SJ, Milan PB, Hooshmand S, Kim HW, Mozafari M. Quantum Dots: a Review from Concept to Clinic. *Biotechnol J.* 2020;15(12):e2000117. doi:10.1002/biot.202000117
65. Wagner AM, Knipe JM, Orive G, Peppas NA. Quantum dots in biomedical applications. *Acta Biomater.* 2019;94:44–63. doi:10.1016/j.actbio.2019.05.022
66. Borovaya M, Horiunova I, Plokhovska S, Pushkarova N, Blume Y, Yemets A. Synthesis, Properties and Bioimaging Applications of Silver-Based Quantum Dots. *Int J Mol Sci.* 2021;22(22):12202. doi:10.3390/ijms222212202
67. Savla R, Taratula O, Garbuzenko O, Minko T. Tumor targeted quantum dot-mucin 1 aptamer-doxorubicin conjugate for imaging and treatment of cancer. *J Control Release off J Control Release Soc.* 2011;153(1):16–22. doi:10.1016/j.jconrel.2011.02.015
68. Yukawa H, Baba Y. In vivo fluorescence imaging and the diagnosis of stem cells using quantum dots for regenerative medicine. *Anal Chem.* 2017;89(5):2671–2681. doi:10.1021/acs.analchem.6b04763
69. Zhang M, Wang Q, Xu Y, Guo L, Lai Z, Li Z. Graphitic carbon nitride quantum dots as analytical probe for viewing sialic acid on the surface of cells and tissues. *Anal Chim Acta.* 2020;1095:204–211. doi:10.1016/j.aca.2019.10.031
70. Zhang WH, Ma W, Long YT. Redox-mediated indirect fluorescence immunoassay for the detection of disease biomarkers using dopamine-functionalized quantum dots. *Anal Chem.* 2016;88(10):5131–5136. doi:10.1021/acs.analchem.6b00048
71. Deng H, Konopka CJ, Prabhu S, et al. Dextran-mimetic quantum dots for multimodal macrophage imaging in vivo, ex vivo, and in situ. *ACS Nano.* 2022;16(2):1999–2012. doi:10.1021/acsnano.1c07010
72. Dong L, Li W, Yu L, Sun L, Chen Y, Hong G. Ultrasmall Ag<sub>2</sub>Te Quantum Dots with Rapid Clearance for Amplified Computed Tomography Imaging and Augmented Photonic Tumor Hyperthermia. *ACS Appl Mater Interfaces.* 2020;12(38):42558–42566. doi:10.1021/acsnano.1c012948
73. Lee YW, Kim M, Kim ZH, Han SW. One-step synthesis of Au@Pd core-shell nanooctahedron. *J Am Chem Soc.* 2009;131(47):17036–17037. doi:10.1021/ja905603p
74. Brito-Silva AM, Sobral-Filho RG, Barbosa-Silva R, de Araújo CB, Galembeck A, Brolo AG. Improved synthesis of gold and silver nanoshells. *Langmuir ACS J Surf Colloids.* 2013;29(13):4366–4372. doi:10.1021/la3050626
75. Liberman A, Wu Z, Barback CV, et al. Color Doppler ultrasound and gamma imaging of intratumorally injected 500 nm iron-silica nanoshells. *ACS Nano.* 2013;7(7):6367–6377. doi:10.1021/nn402507d
76. Song J, Yang X, Yang Z, et al. Rational Design of Branched Nanoporous Gold Nanoshells with Enhanced Physico-Optical Properties for Optical Imaging and Cancer Therapy. *ACS Nano.* 2017;11(6):6102–6113. doi:10.1021/acsnano.7b02048
77. He J, Qiao Y, Zhang H, et al. Gold-silver nanoshells promote wound healing from drug-resistant bacteria infection and enable monitoring via surface-enhanced Raman scattering imaging. *Biomaterials.* 2020;234:119763. doi:10.1016/j.biomaterials.2020.119763
78. He J, Wei Q, Wang S, Hua S, Zhou M. Bioinspired protein Corona strategy enhanced biocompatibility of Ag-Hybrid hollow Au nanoshells for surface-enhanced Raman scattering imaging and on-demand activation tumor-phototherapy. *Biomaterials.* 2021;271:120734. doi:10.1016/j.biomaterials.2021.120734
79. Coughlin AJ, Ananta JS, Deng N, Larina IV, Decuzzi P, West JL. Gadolinium-conjugated gold nanoshells for multimodal diagnostic imaging and photothermal cancer therapy. *Small Weinh Bergstr Ger.* 2014;10(3):556–565. doi:10.1002/sml.201302217
80. Tuersun P, Han X. Optimal dimensions of gold nanoshells for light backscattering and absorption based applications. *J Quant Spectrosc Radiat Transf.* 2014;146:468–474. doi:10.1016/j.jqsrt.2013.12.018
81. Ahmadi A, Arami S. Potential applications of nanoshells in biomedical sciences. *J Drug Target.* 2014;22(3):175–190. doi:10.3109/1061186X.2013.839684
82. Ye Y, Chen X. Integrin targeting for tumor optical imaging. *Theranostics.* 2011;1:102–126. doi:10.7150/thno/v01p0102
83. Cha MG, Kang H, Choi YS, et al. Effect of Alkylamines on Morphology Control of Silver Nanoshells for Highly Enhanced Raman Scattering. *ACS Appl Mater Interfaces.* 2019;11(8):8374–8381. doi:10.1021/acsnano.8b15674
84. Li L, Jiang R, Shan B, Lu Y, Zheng C, Li M. Near-infrared II plasmonic porous cubic nanoshells for in vivo noninvasive SERS visualization of sub-millimeter microtumors. *Nat Commun.* 2022;13(1):5249. doi:10.1038/s41467-022-32975-w

85. Yasun E, Gandhi S, Choudhury S, et al. Hollow micro and nanostructures for therapeutic and imaging applications. *J Drug Deliv Sci Technol.* 2020;60:102094. doi:10.1016/j.jddst.2020.102094
86. Caminade AM, Yan D, Smith DK. Dendrimers and hyperbranched polymers. *Chem Soc Rev.* 2015;44(12):3870–3873. doi:10.1039/C5CS90049B
87. Lee DE, Koo H, Sun IC, Ryu JH, Kim K, Kwon IC. Multifunctional nanoparticles for multimodal imaging and theragnosis. *Chem Soc Rev.* 2012;41(7):2656–2672. doi:10.1039/C2CS15261D
88. Carvalho MR, Reis RL, Oliveira JM. Dendrimer nanoparticles for colorectal cancer applications. *J Mater Chem B.* 2020;8(6):1128–1138. doi:10.1039/C9TB02289A
89. Menjoge AR, Kannan RM, Tomalia DA. Dendrimer-based drug and imaging conjugates: design considerations for nanomedical applications. *Drug Discov Today.* 2010;15(5–6):171–185. doi:10.1016/j.drudis.2010.01.009
90. Markowicz-Piasecka M, Sikora J, Szymański P, Kozak O, Studniarek M, Mikiciuk-Olasik E. PAMAM dendrimers as potential carriers of gadolinium complexes of iminodiacetic acid derivatives for magnetic resonance imaging. *J Nanomater.* 2015;16(1):26. doi:10.1155/2015/394827
91. Ali ES, Sharker S, Islam MT, et al. Targeting cancer cells with nanotherapeutics and nanodiagnostics: current status and future perspectives. *Semin Cancer Biol.* 2021;69:52–68. doi:10.1016/j.semcancer.2020.01.011
92. Li H, Wang P, Gong W, et al. Dendron-Grafted Polylysine-Based Dual-Modal Nanoprobe for Ultra-Early Diagnosis of Pancreatic Precancerosis via Targeting a Urokinase-Type Plasminogen Activator Receptor. *Adv Healthc Mater.* 2018;7(5). doi:10.1002/adhm.201700912
93. Mekuria SL, Debele TA, Tsai HC. PAMAM dendrimer based targeted nano-carrier for bio-imaging and therapeutic agents. *Rsc Adv.* 2016;6(68):63761–63772. doi:10.1039/C6RA12895E
94. Palmerston Mendes L, Pan J, Torchilin VP. Dendrimers as nanocarriers for nucleic acid and drug delivery in cancer therapy. *Molecules.* 2017;22(9):1401. doi:10.3390/molecules22091401
95. Xing Y, Zhu J, Zhao L, et al. SPECT/CT imaging of chemotherapy-induced tumor apoptosis using <sup>99m</sup>Tc-labeled dendrimer-entrapped gold nanoparticles. *Drug Deliv.* 2018;25(1):1384–1393. doi:10.1080/10717544.2018.1474968
96. Hernández-Rivera M, Zaibac NG, Wilson LJ. Toward carbon nanotube-based imaging agents for the clinic. *Biomaterials.* 2016;101:229–240. doi:10.1016/j.biomaterials.2016.05.045
97. Treacy MMJ, Ebbesen TW, Gibson JM. Exceptionally high Young's modulus observed for individual carbon nanotubes. *Nature.* 1996;381(6584):678–680. doi:10.1038/381678a0
98. Carlson LJ, Krauss TD. Photophysics of individual single-walled carbon nanotubes. *Acc Chem Res.* 2008;41(2):235–243. doi:10.1021/ar700136v
99. Salem DP, Gong X, Liu AT, Koman VB, Dong J, Strano MS. Ionic Strength-Mediated Phase Transitions of Surface-Adsorbed DNA on Single-Walled Carbon Nanotubes. *J Am Chem Soc.* 2017;139(46):16791–16802. doi:10.1021/jacs.7b09258
100. Bartelmess J, Quinn SJ, Giordani S. Carbon nanomaterials: multi-functional agents for biomedical fluorescence and Raman imaging. *Chem Soc Rev.* 2015;44(14):4672–4698. doi:10.1039/c4cs00306c
101. Welsher K, Sherlock SP, Dai H. Deep-tissue anatomical imaging of mice using carbon nanotube fluorophores in the second near-infrared window. *Proc Natl Acad Sci U S A.* 2011;108(22):8943–8948. doi:10.1073/pnas.1014501108
102. Rivera EJ, Tran LA, Hernández-Rivera M, et al. Bismuth@US-tubes as a Potential Contrast Agent for X-ray Imaging Applications. *J Mater Chem B Mater Biol Med.* 2013;1(37):10.1039/C3TB20742K. doi:10.1039/C3TB20742K
103. Kukreja A, Kang B, Kim HO, et al. Preparation of gold core-mesoporous iron-oxide shell nanoparticles and their application as dual MR/CT contrast agent in human gastric cancer cells. *J Ind Eng Chem.* 2017;48:56–65. doi:10.1016/j.jiec.2016.12.020
104. Alkilany AM, Lohse SE, Murphy CJ. The Gold Standard: gold Nanoparticle Libraries To Understand the Nano–Bio Interface. *Acc Chem Res.* 2013;46(3):650–661. doi:10.1021/ar300015b
105. Khan AK, Rashid R, Murtaza G, Zahra A. Gold nanoparticles: synthesis and applications in drug delivery. *Trop J Pharm Res.* 2014;13(7):1169–1177. doi:10.4314/tjpr.v13i7.23
106. Black KCL, Yi J, Rivera JG, Zelasko-Leon DC, Messersmith PB. Polydopamine-enabled surface functionalization of gold nanorods for cancer cell-targeted imaging and photothermal therapy. *Nanomed.* 2013;8(1):17–28. doi:10.2217/nnm.12.82
107. Puvanakrishnan P, Park J, Diagaradjane P, et al. Near-infrared narrow-band imaging of gold/silica nanoshells in tumors. *J Biomed Opt.* 2009;14(2):024044. doi:10.1117/1.3120494
108. Wu Y, Ali MRK, Chen K, Fang N, El-Sayed MA. Gold nanoparticles in biological optical imaging. *Nano Today.* 2019;24:120–140. doi:10.1016/j.nantod.2018.12.006
109. Panahi Y, Mohammadhosseini M, Nejati-Koshki K, et al. Preparation, Surface Properties, and Therapeutic Applications of Gold Nanoparticles in Biomedicine. *Drug Res.* 2017;67(2):77–87. doi:10.1055/s-0042-115171
110. Alagaratnam S, Yang SY, Loizidou M, Fuller B, Ramesh B. Mechano-growth Factor Expression in Colorectal Cancer Investigated With Fluorescent Gold Nanoparticles. *Anticancer Res.* 2019;39(4):1705–1710. doi:10.21873/anticancer.13276
111. Muhammad M, sheng SC, Huang Q. Aptamer-functionalized Au nanoparticles array as the effective SERS biosensor for label-free detection of interleukin-6 in serum. *Sens Actuators B Chem.* 2021;334:129607. doi:10.1016/j.snb.2021.129607
112. Meir R, Shamalov K, Betzer O, et al. Nanomedicine for Cancer Immunotherapy: tracking Cancer-Specific T-Cells in Vivo with Gold Nanoparticles and CT Imaging. *ACS Nano.* 2015;9(6):6363–6372. doi:10.1021/acsnano.5b01939
113. Ding P, Chen L, Wei C, et al. Efficient Synthesis of Stable Polyelectrolyte Complex Nanoparticles by Electrostatic Assembly Directed Polymerization. *Macromol Rapid Commun.* 2021;42(4):2000635. doi:10.1002/marc.202000635
114. Sing E. Recent progress in the science of complex coacervation. *Soft Matter.* 2020;16(12):2885–2914. doi:10.1039/D0SM00001A
115. Sing CE. Development of the modern theory of polymeric complex coacervation. *Adv Colloid Interface Sci.* 2017;239:2–16. doi:10.1016/j.cis.2016.04.004
116. Liu Z, Jiao Y, Wang Y, Zhou C, Zhang Z. Polysaccharides-based nanoparticles as drug delivery systems. *Adv Drug Deliv Rev.* 2008;60(15):1650–1662. doi:10.1016/j.addr.2008.09.001
117. Müller M, Keßler B, Fröhlich J, Poeschla S, Torger B. Polyelectrolyte Complex Nanoparticles of Poly(ethyleneimine) and Poly(acrylic acid): preparation and Applications. *Polymers.* 2011;3(2):762–778. doi:10.3390/polym3020762

118. Schatz C, Lucas JM, Viton C, Domard A, Pichot C, Delair T. Formation and Properties of Positively Charged Colloids Based on Polyelectrolyte Complexes of Biopolymers. *Langmuir*. 2004;20(18):7766–7778. doi:10.1021/la049460m
119. Meka VS, Sing MKG, Pichika MR, Nali SR, Kolapalli VRM, Kesharwani P. A comprehensive review on polyelectrolyte complexes. *Drug Discov Today*. 2017;22(11):1697–1706. doi:10.1016/j.drudis.2017.06.008
120. Deng L, Dong H, Dong A, Zhang J. A strategy for oral chemotherapy via dual pH-sensitive polyelectrolyte complex nanoparticles to achieve gastric survivability, intestinal permeability, hemodynamic stability and intracellular activity. *Eur J Pharm Biopharm*. 2015;97:107–117. doi:10.1016/j.ejpb.2015.10.010
121. Mohanta BC, Javed MN, Hasnain MS, Nayak AK. Chapter 12 - Polyelectrolyte complexes of alginate for controlling drug release. In: Nayak AK, Hasnain MS editors. *Alginates in Drug Delivery*. Academic Press; 2020:297–321. doi:10.1016/B978-0-12-817640-5.00012-1.
122. De R, Han Song Y. pH-responsive polyelectrolyte complexation on upconversion nanoparticles: a multifunctional nanocarrier for protection, delivery, and 3D-imaging of therapeutic protein. *J Mater Chem B*. 2022;10(18):3420–3433. doi:10.1039/D2TB00246A
123. Ai H. Layer-by-layer capsules for magnetic resonance imaging and drug delivery. *Adv Drug Deliv Rev*. 2011;63(9):772–788. doi:10.1016/j.addr.2011.03.013
124. Huang M, Huang ZL, Bilgen M, Berkland C. Magnetic resonance imaging of contrast-enhanced polyelectrolyte complexes. *Nanomed Nanotechnol Biol Med*. 2008;4(1):30–40. doi:10.1016/j.nano.2007.10.085
125. Berret JF, Schonbeck N, Gazeau F, et al. Controlled clustering of superparamagnetic nanoparticles using block copolymers: design of new contrast agents for magnetic resonance imaging. *J Am Chem Soc*. 2006;128(5):1755–1761. doi:10.1021/ja0562999
126. Barth BM, Sharma R, Altinoğlu EI, et al. Bioconjugation of calcium phosphosilicate composite nanoparticles for selective targeting of human breast and pancreatic cancers in vivo. *ACS Nano*. 2010;4(3):1279–1287. doi:10.1021/nn901297q
127. Iafisco M, Degli Esposti L, Ramirez-Rodríguez GB, et al. Fluoride-doped amorphous calcium phosphate nanoparticles as a promising biomimetic material for dental remineralization. *Sci Rep*. 2018;8(1):17016. doi:10.1038/s41598-018-35258-x
128. Khalifehzadeh R, Arami H. Biodegradable calcium phosphate nanoparticles for cancer therapy. *Adv Colloid Interface Sci*. 2020;279:102157. doi:10.1016/j.cis.2020.102157
129. Huang D, He B, Mi P. Calcium phosphate nanocarriers for drug delivery to tumors: imaging, therapy and theranostics. *Biomater Sci*. 2019;7(10):3942–3960. doi:10.1039/C9BM00831D
130. Qi C, Lin J, Fu LH, Huang P. Calcium-based biomaterials for diagnosis, treatment, and theranostics. *Chem Soc Rev*. 2018;47(2):357–403. doi:10.1039/c6cs00746e
131. Huang KW, Hsu FF, Qiu JT, et al. Highly efficient and tumor-selective nanoparticles for dual-targeted immunogene therapy against cancer. *Sci Adv*. 2020;6(3):eaax5032. doi:10.1126/sciadv.aax5032
132. Khalifehzadeh R, Arami H. The CpG molecular structure controls the mineralization of calcium phosphate nanoparticles and their immunostimulation efficacy as vaccine adjuvants. *Nanoscale*. 2020;12(17):9603–9615. doi:10.1039/c9nr09782a
133. Zhang NN, Lu CY, Shu GF, et al. Gadolinium-loaded calcium phosphate nanoparticles for magnetic resonance imaging of orthotopic hepatocarcinoma and primary hepatocellular carcinoma. *Biomater Sci*. 2020;8(7):1961–1972. doi:10.1039/c9bm01544b
134. Mi P, Kokuryo D, Cabral H, et al. A pH-activatable nanoparticle with signal-amplification capabilities for non-invasive imaging of tumour malignancy. *Nat Nanotechnol*. 2016;11(8):724–730. doi:10.1038/nnano.2016.72
135. Wu L, Liu F, Liu S, Xu X, Liu Z. Perfluorocarbons-Based <sup>19</sup>F Magnetic Resonance Imaging in Biomedicine. *Int J Nanomedicine*. 2020;15:7377–7395. doi:10.2147/IJN.S255084
136. Yang Q, Li P, Ran H, et al. Polypyrrole-coated phase-change liquid perfluorocarbon nanoparticles for the visualized photothermal-chemotherapy of breast cancer. *Acta Biomater*. 2019;90:337–349. doi:10.1016/j.actbio.2019.03.056
137. Koshkina O, Lajoinie G, Bombelli FB, et al. Multicore Liquid Perfluorocarbon-Loaded Multimodal Nanoparticles for Stable Ultrasound and <sup>19</sup>F MRI Applied to In Vivo Cell Tracking. *Adv Funct Mater*. 2019;29(19):1806485. doi:10.1002/adfm.201806485
138. Shin SH, Kadayakkara DK, Bulte JWM. In Vivo <sup>19</sup>F MR Imaging Cell Tracking of Inflammatory Macrophages and Site-specific Development of Colitis-associated Dysplasia. *Radiology*. 2017;282(1):194–201. doi:10.1148/radiol.2016152387
139. Mulder WJM, Strijkers GJ, van Tilborg GAF, Cormode DP, Fayad ZA, Nicolay K. Nanoparticulate Assemblies of Amphiphiles and Diagnostically Active Materials for Multimodality Imaging. *Acc Chem Res*. 2009;42(7):904–914. doi:10.1021/ar800223c
140. Shah S, Dhawan V, Holm R, Nagarsenker MS, Perrie Y. Liposomes: advancements and innovation in the manufacturing process. *Adv Drug Deliv Rev*. 2020;154-155:102–122. doi:10.1016/j.addr.2020.07.002
141. Younis NK, Roumieh R, Bassil EP, Ghoubaire JA, Kobeissy F, Eid AH. Nanoparticles: attractive tools to treat colorectal cancer. *Semin Cancer Biol*. 2022;86(Pt 2):1–13. doi:10.1016/j.semcancer.2022.08.006
142. Tan C, Wang J, Sun B. Biopolymer-liposome hybrid systems for controlled delivery of bioactive compounds: recent advances. *Biotechnol Adv*. 2021;48:107727. doi:10.1016/j.biotechadv.2021.107727
143. Li T, Cipolla D, Rades T, Boyd BJ. Drug nanocrystallisation within liposomes. *J Control Release off J Control Release Soc*. 2018;288:96–110. doi:10.1016/j.jconrel.2018.09.001
144. Large DE, Abdelmessih RG, Fink EA, Auguste DT. Liposome composition in drug delivery design, synthesis, characterization, and clinical application. *Adv Drug Deliv Rev*. 2021;176:113851. doi:10.1016/j.addr.2021.113851
145. Thébault CJ, Ramniceanu G, Michel A, et al. In Vivo Evaluation of Magnetic Targeting in Mice Colon Tumors with Ultra-Magnetic Liposomes Monitored by MRI. *Mol Imaging Biol*. 2019;21(2):269–278. doi:10.1007/s11307-018-1238-3
146. Awad NS, Haider M, Paul V, et al. Ultrasound-Triggered Liposomes Encapsulating Quantum Dots as Safe Fluorescent Markers for Colorectal Cancer. *Pharmaceutics*. 2021;13(12):2073. doi:10.3390/pharmaceutics13122073
147. Petersen AL, Hansen AE, Gabizon A, Andresen TL. Liposome imaging agents in personalized medicine. *Adv Drug Deliv Rev*. 2012;64(13):1417–1435. doi:10.1016/j.addr.2012.09.003
148. Dams ET, Oyen WJ, Boerman OC, et al. Technetium-99m-labeled liposomes to image experimental colitis in rabbits: comparison with technetium-99m-HMPAO-granulocytes and technetium-99m-HYNIC-IgG. *J Nucl Med off Publ Soc Nucl Med*. 1998;39(12):2172–2178.
149. Blocker SJ, Douglas KA, Polin LA, et al. Liposomal <sup>64</sup>Cu-PET Imaging of Anti-VEGF Drug Effects on Liposomal Delivery to Colon Cancer Xenografts. *Theranostics*. 2017;7(17):4229–4239. doi:10.7150/thno.21688
150. Torchilin VP. Micellar Nanocarriers: pharmaceutical Perspectives. *Pharm Res*. 2007;24(1):1–16. doi:10.1007/s11095-006-9132-0

151. Biswas S, Kumari P, Lakhani PM, Ghosh B. Recent advances in polymeric micelles for anti-cancer drug delivery. *Eur J Pharm Sci.* 2016;83:184–202. doi:10.1016/j.ejps.2015.12.031
152. Takashima H, Koga Y, Tsumura R, et al. Reinforcement of antitumor effect of micelles containing anticancer drugs by binding of an anti-tissue factor antibody without direct cytotoxic effects. *J Control Release off J Control Release Soc.* 2020;323:138–150. doi:10.1016/j.jconrel.2020.03.048
153. Lin M, Dai Y, Xia F, Zhang X. Advances in non-covalent crosslinked polymer micelles for biomedical applications. *Mater Sci Eng C Mater Biol Appl.* 2021;119:111626. doi:10.1016/j.msec.2020.111626
154. Movassaghian S, Merkel OM, Torchilin VP. Applications of polymer micelles for imaging and drug delivery. *Wiley Interdiscip Rev Nanomed Nanobiotechnol.* 2015;7(5):691–707. doi:10.1002/wnan.1332
155. Torchilin VP. Polymeric contrast agents for medical imaging. *Curr Pharm Biotechnol.* 2000;1(2):183–215. doi:10.2174/1389201003378960
156. Zhang Y, Wang D, Goel S, et al. Surfactant-Stripped Frozen Pheophytin Micelles for Multimodal Gut Imaging. *Adv Mater Deerfield Beach Fla.* 2016;28(38):8524–8530. doi:10.1002/adma.201602373
157. Jiang Z, Sun B, Wang Y, et al. Surfactant-Stripped Micelles with Aggregation-Induced Enhanced Emission for Bimodal Gut Imaging In Vivo and Microbiota Tagging Ex Vivo. *Adv Healthc Mater.* 2021;10(24):e2100356. doi:10.1002/adhm.202100356
158. Haase M, Schäfer H. Upconverting nanoparticles. *Angew Chem Int Ed Engl.* 2011;50(26):5808–5829. doi:10.1002/anie.201005159
159. Chen G, Qiu H, Prasad PN, Chen X. Upconversion Nanoparticles: design, Nanochemistry, and Applications in Theranostics. *Chem Rev.* 2014;114(10):5161–5214. doi:10.1021/cr400425h
160. Jalani G, Tam V, Vetrone F, Cerruti M. Seeing, Targeting and Delivering with Upconverting Nanoparticles. *J Am Chem Soc.* 2018;140(35):10923–10931. doi:10.1021/jacs.8b03977
161. Wu S, Butt HJ. Near-Infrared-Sensitive Materials Based on Upconverting Nanoparticles. *Adv Mater Deerfield Beach Fla.* 2016;28(6):1208–1226. doi:10.1002/adma.201502843
162. Auzel F. Upconversion and anti-stokes processes with f and d ions in solids. *Chem Rev.* 2004;104(1):139–173. doi:10.1021/cr020357g
163. Wu S, Han G, Milliron DJ, et al. Non-blinking and photostable upconverted luminescence from single lanthanide-doped nanocrystals. *Proc Natl Acad Sci U S A.* 2009;106(27):10917–10921. doi:10.1073/pnas.0904792106
164. Hou Z, Zhang Y, Deng K, et al. UV-emitting upconversion-based TiO<sub>2</sub> photosensitizing nanoplateform: near-infrared light mediated in vivo photodynamic therapy via mitochondria-involved apoptosis pathway. *ACS Nano.* 2015;9(3):2584–2599. doi:10.1021/nn506107c
165. Dong H, Du SR, Zheng XY, et al. Lanthanide Nanoparticles: from Design toward Bioimaging and Therapy. *Chem Rev.* 2015;115(19):10725–10815. doi:10.1021/acs.chemrev.5b00091
166. Wang Z, Liu C, Zhao Y, et al. Photomagnetic nanoparticles in dual-modality imaging and photo-sonodynamic activity against bacteria. *Chem Eng J.* 2019;356:811–818. doi:10.1016/j.cej.2018.09.077
167. Li Z, Lv S, Wang Y, Chen S, Liu Z. Construction of LRET-Based Nanoprobe Using Upconversion Nanoparticles with Confined Emitters and Bared Surface as Luminophore. *J Am Chem Soc.* 2015;137(9):3421–3427. doi:10.1021/jacs.5b01504
168. Berezin MY, Achilefu S. Fluorescence lifetime measurements and biological imaging. *Chem Rev.* 2010;110(5):2641–2684. doi:10.1021/cr900343z
169. Tian R, Zhao S, Liu G, et al. Construction of lanthanide-doped upconversion nanoparticle-Ulex Europaeus Agglutinin-I bioconjugates with brightness red emission for ultrasensitive in vivo imaging of colorectal tumor. *Biomaterials.* 2019;212:64–72. doi:10.1016/j.biomaterials.2019.05.010
170. Chu Z, Guo J, Guo J. Up-Conversion Luminescence System for Quantitative Detection of IL-6. *IEEE Trans Nanobioscience.* 2023;22(2):203–211. doi:10.1109/TNB.2022.3178754
171. Rogalla S, Flisikowski K, Gorpas D, et al. Biodegradable fluorescent nanoparticles for endoscopic detection of colorectal carcinogenesis. *Adv Funct Mater.* 2019;29(51):1904992. doi:10.1002/adfm.201904992
172. da Paz MC, Santos M, Santos CMB, et al. Anti-CEA loaded maghemite nanoparticles as a theragnostic device for colorectal cancer. *Int J Nanomedicine.* 2012;7:5271–5282. doi:10.2147/IJN.S32139
173. Wang Q, Chen E, Cai Y, et al. Preoperative endoscopic localization of colorectal cancer and tracing lymph nodes by using carbon nanoparticles in laparoscopy. *World J Surg Oncol.* 2016;14(1):231. doi:10.1186/s12957-016-0987-1
174. Lin D, Feng S, Pan J, et al. Colorectal cancer detection by gold nanoparticle based surface-enhanced Raman spectroscopy of blood serum and statistical analysis. *Opt Express.* 2011;19(14):13565–13577. doi:10.1364/OE.19.013565
175. Sun J, Zhang S, Jiang S, et al. Gadolinium-Loaded Solid Lipid Nanoparticles as a Tumor-Absorbable Contrast Agent for Early Diagnosis of Colorectal Tumors Using Magnetic Resonance Colonography. *J Biomed Nanotechnol.* 2016;12(9):1709–1723. doi:10.1166/jbn.2016.2285
176. Park Y, Ryu YM, Jung Y, et al. Spraying quantum dot conjugates in the colon of live animals enabled rapid and multiplex cancer diagnosis using endoscopy. *ACS Nano.* 2014;8(9):8896–8910. doi:10.1021/nn5009269
177. Kolitz-Domb M, Corem-Salkmon E, Grinberg I, Margel S. Synthesis and characterization of bioactive conjugated near-infrared fluorescent proteinoid-poly(L-lactic acid) hollow nanoparticles for optical detection of colon cancer. *Int J Nanomedicine.* 2014;9:5041–5053. doi:10.2147/IJN.S68582
178. Harmsen S, Rogalla S, Huang R, et al. Detection of Premalignant Gastrointestinal Lesions Using Surface-Enhanced Resonance Raman Scattering-Nanoparticle Endoscopy. *ACS Nano.* 2019;13(2):1354–1364. doi:10.1021/acsnano.8b06808
179. Montet X, Pastor CM, Vallée JP, et al. Improved visualization of vessels and hepatic tumors by micro-computed tomography (CT) using iodinated liposomes. *Invest Radiol.* 2007;42(9):652–658. doi:10.1097/RLI.0b013e31805f445b
180. Liu H, Wang H, Xu Y, et al. Lactobionic acid-modified dendrimer-entrapped gold nanoparticles for targeted computed tomography imaging of human hepatocellular carcinoma. *ACS Appl Mater Interfaces.* 2014;6(9):6944–6953. doi:10.1021/am500761x
181. Zhou B, Xiong Z, Wang P, Peng C, Shen M, Shi X. Acetylated Polyethylenimine-Entrapped Gold Nanoparticles Enable Negative Computed Tomography Imaging of Orthotopic Hepatic Carcinoma. *Langmuir ACS J Surf Colloids.* 2018;34(29):8701–8707. doi:10.1021/acs.langmuir.8b01669
182. Li J, Cha R, Zhang Y, et al. Iron oxide nanoparticles for targeted imaging of liver tumors with ultralow hepatotoxicity. *J Mater Chem B.* 2018;6(40):6413–6423. doi:10.1039/C8TB01657G



183. Wu S, Meng X, Jiang X, et al. Harnessing X-Ray Energy-Dependent Attenuation of Bismuth-Based Nanoprobes for Accurate Diagnosis of Liver Fibrosis. *Adv Sci Weinh Baden-Wurt Ger.* 2021;8(11):e2002548. doi:10.1002/adv.202002548
184. Wang X, Wang J, Pan J, et al. Rhenium Sulfide Nanoparticles as a Biosafe Spectral CT Contrast Agent for Gastrointestinal Tract Imaging and Tumor Theranostics in Vivo. *ACS Appl Mater Interfaces.* 2019;11(37):33650–33658. doi:10.1021/acsami.9b10479
185. Fan X, Wang L, Guo Y, et al. Experimental investigation of the penetration of ultrasound nanobubbles in a gastric cancer xenograft. *Nanotechnology.* 2013;24(32):325102. doi:10.1088/0957-4484/24/32/325102
186. Shang W, Xia X, Lu N, et al. Colourful fluorescence-based carbon dots for tumour imaging-guided nanosurgery. *Nanomed Nanotechnol Biol Med.* 2022;45:102583. doi:10.1016/j.nano.2022.102583
187. Naha PC, Hsu JC, Kim J, et al. Dextran-Coated Cerium Oxide Nanoparticles: a Computed Tomography Contrast Agent for Imaging the Gastrointestinal Tract and Inflammatory Bowel Disease. *ACS Nano.* 2020;14(8):10187–10197. doi:10.1021/acsnano.0c03457
188. Mi C, Guan M, Zhang X, et al. High Spatial and Temporal Resolution NIR-IIb Gastrointestinal Imaging in Mice. *Nano Lett.* 2022;22(7):2793–2800. doi:10.1021/acs.nanolett.1c04909
189. Zhao S, Wang S, Pan P, et al. Magnitude, Risk Factors, and Factors Associated With Adenoma Miss Rate of Tandem Colonoscopy: a Systematic Review and Meta-analysis. *Gastroenterology.* 2019;156(6):1661–1674.e11. doi:10.1053/j.gastro.2019.01.260
190. Iacucci M, Furfaro F, Matsumoto T, et al. Advanced endoscopic techniques in the assessment of inflammatory bowel disease: new technology, new era. *Gut.* 2019;68(3):562–572. doi:10.1136/gutjnl-2017-315235
191. Chiu HM, Chang CY, Chen CC, et al. A prospective comparative study of narrow-band imaging, chromoendoscopy, and conventional colonoscopy in the diagnosis of colorectal neoplasia. *Gut.* 2007;56(3):373–379. doi:10.1136/gut.2006.099614
192. Hu Z, Chen WH, Tian J, Cheng Z. NIRF Nanoprobes for Cancer Molecular Imaging: approaching Clinic. *Trends Mol Med.* 2020;26(5):469–482. doi:10.1016/j.molmed.2020.02.003
193. Frangioni JV. In vivo near-infrared fluorescence imaging. *Curr Opin Chem Biol.* 2003;7(5):626–634. doi:10.1016/j.cbpa.2003.08.007
194. Yi X, Wang F, Qin W, Yang X, Yuan J. Near-infrared fluorescent probes in cancer imaging and therapy: an emerging field. *Int J Nanomedicine.* 2014;9:1347–1365. doi:10.2147/IJN.S60206
195. T H, L K, W W. Near-infrared fluorescent probes for imaging of amyloid plaques in Alzheimer's disease. *Acta Pharm Sin B.* 2015;5(1). doi:10.1016/j.apsb.2014.12.006
196. Miao Q, Pu K. Organic Semiconducting Agents for Deep-Tissue Molecular Imaging: second Near-Infrared Fluorescence, Self-Luminescence, and Photoacoustics. *Adv Mater Deerfield Beach Fla.* 2018;30(49):e1801778. doi:10.1002/adma.201801778
197. Levesque E, Martin E, Dudau D, Lim C, Dhonneur G, Azoulay D. Current use and perspective of indocyanine green clearance in liver diseases. *Anaesth Crit Care Pain Med.* 2016;35(1):49–57. doi:10.1016/j.accpm.2015.06.006
198. Wang H, Li X, Tse BWC, et al. Indocyanine green-incorporating nanoparticles for cancer theranostics. *Theranostics.* 2018;8(5):1227–1242. doi:10.7150/thno.22872
199. Wang YW, Fu YY, Peng Q, et al. Dye-enhanced graphene oxide for photothermal therapy and photoacoustic imaging. *J Mater Chem B.* 2013;1(42):5762–5767. doi:10.1039/c3tb20986e
200. Egloff-Juras C, Bezdetnaya L, Dolivet G, Lassalle HP. NIR fluorescence-guided tumor surgery: new strategies for the use of indocyanine green. *Int J Nanomedicine.* 2019;14:7823–7838. doi:10.2147/IJN.S207486
201. Jokerst JV, Gambhir SS. Molecular Imaging with Theranostic Nanoparticles. *Acc Chem Res.* 2011;44(10):1050–1060. doi:10.1021/ar200106e
202. Pellach M, Grinberg I, Margel S. Near IR fluorescent polystyrene/albumin core/shell nanoparticles for specific targeting of colonic neoplasms. *Macromol Biosci.* 2012;12(11):1472–1479. doi:10.1002/mabi.201200142
203. Tiernan JP, Ingram N, Marston G, et al. CEA-targeted nanoparticles allow specific in vivo fluorescent imaging of colorectal cancer models. *Nanomed.* 2015;10(8):1223–1231. doi:10.2217/nnm.14.202
204. Xu G, Yan Q, Lv X, et al. Imaging of Colorectal Cancers Using Activatable Nanoprobes with Second Near-Infrared Window Emission. *Angew Chem Int Ed Engl.* 2018;57(14):3626–3630. doi:10.1002/anie.201712528
205. Gournaris E, Park W, Cho S, Bentrem DJ, Larson AC, Kim DH. Near-Infrared Fluorescent Endoscopic Image-Guided Photothermal Ablation Therapy of Colorectal Cancer Using Dual-Modal Gold Nanorods Targeting Tumor-Infiltrating Innate Immune Cells in a Transgenic TS4 CRE/APCloxΔ468 Mouse Model. *ACS Appl Mater Interfaces.* 2019;11(24):21353–21359. doi:10.1021/acsami.9b04186
206. Liu Y, Ai K, Lu L. Nanoparticulate X-ray computed tomography contrast agents: from design validation to in vivo applications. *Acc Chem Res.* 2012;45(10):1817–1827. doi:10.1021/ar300150c
207. Ahmed EA, Abdelatty K, Mahdy RE, Emara DM, Header DA. Computed tomography enterocolonography in assessment of degree of ulcerative colitis activity. *Int J Clin Pract.* 2021;75(10):e14626. doi:10.1111/ijcp.14626
208. Singh J, Daftary A. Iodinated contrast media and their adverse reactions. *J Nucl Med Technol.* 2008;36(2):69–74; quiz 76–77. doi:10.2967/jnm.107.047621
209. Wang CL, Cohan RH, Ellis JH, Adusumilli S, Dunnick NR. Frequency, management, and outcome of extravasation of nonionic iodinated contrast medium in 69,657 intravenous injections. *Radiology.* 2007;243(1):80–87. doi:10.1148/radiol.2431060554
210. Lee N, Choi SH, Hyeon T. Nano-sized CT contrast agents. *Adv Mater Deerfield Beach Fla.* 2013;25(19):2641–2660. doi:10.1002/adma.201300081
211. Cheheltani R, Ezzibdeh RM, Chhour P, et al. Tunable, biodegradable gold nanoparticles as contrast agents for computed tomography and photoacoustic imaging. *Biomaterials.* 2016;102:87–97. doi:10.1016/j.biomaterials.2016.06.015
212. Hsu JC, Nieves LM, Betzer O, et al. Nanoparticle contrast agents for X-ray imaging applications. *Wiley Interdiscip Rev Nanomed Nanobiotechnol.* 2020;12(6):e1642. doi:10.1002/wnan.1642
213. Han X, Xu K, Taratula O, Farsad K. Applications of nanoparticles in biomedical imaging. *Nanoscale.* 2019;11(3):799–819. doi:10.1039/c8nr07769j
214. Li X, Anton N, Zuber G, et al. Iodinated  $\alpha$ -tocopherol nano-emulsions as non-toxic contrast agents for preclinical X-ray imaging. *Biomaterials.* 2013;34(2):481–491. doi:10.1016/j.biomaterials.2012.09.026
215. Zou Y, Wei Y, Wang G, et al. Nanopolymerosomes with an Ultrahigh Iodine Content for High-Performance X-Ray Computed Tomography Imaging In Vivo. *Adv Mater Deerfield Beach Fla.* 2017;29(10). doi:10.1002/adma.201603997

216. Meng X, Wu Y, Bu W. Functional CT Contrast Nanoagents for the Tumor Microenvironment. *Adv Healthc Mater.* 2021;10(5):e2000912. doi:10.1002/adhm.202000912
217. Zhang P, Ma X, Guo R, et al. Organic Nanoplatforams for Iodinated Contrast Media in CT Imaging. *Mol Basel Switz.* 2021;26(23):7063. doi:10.3390/molecules26237063
218. You S, Jung HY, Lee C, et al. High-performance dendritic contrast agents for X-ray computed tomography imaging using potent tetraiodo-benzene derivatives. *J Control Release off J Control Release Soc.* 2016;226:258–267. doi:10.1016/j.jconrel.2016.01.036
219. Sun Y, Li B, Cao Q, Liu T, Li J. Targeting cancer stem cells with polymer nanoparticles for gastrointestinal cancer treatment. *Stem Cell Res Ther.* 2022;13(1):489. doi:10.1186/s13287-022-03180-9
220. Cole LE, Ross RD, Tilley JM, Vargo-Gogola T, Roeder RK. Gold nanoparticles as contrast agents in x-ray imaging and computed tomography. *Nanomed.* 2015;10(2):321–341. doi:10.2217/nnm.14.171
221. Li Z, Liu J, Hu Y, et al. Biocompatible PEGylated bismuth nanocrystals: All-in-one theranostic agent with triple-modal imaging and efficient in vivo photothermal ablation of tumors. *Biomaterials.* 2017;141:284–295. doi:10.1016/j.biomaterials.2017.06.033
222. He F, Ji H, Feng L, et al. Construction of thiol-capped ultrasmall Au-Bi bimetallic nanoparticles for X-ray CT imaging and enhanced antitumor therapy efficiency. *Biomaterials.* 2021;264:120453. doi:10.1016/j.biomaterials.2020.120453
223. Zelepukin IV, Ivanov IN, Mirkasymov AB, et al. Polymer-coated BiOCl nanosheets for safe and regioselective gastrointestinal X-ray imaging. *J Control Release off J Control Release Soc.* 2022;349:475–485. doi:10.1016/j.jconrel.2022.07.007
224. Luo XF, Xie XQ, Cheng S, et al. Dual-Energy CT for Patients Suspected of Having Liver Iron Overload: can Virtual Iron Content Imaging Accurately Quantify Liver Iron Content? *Radiology.* 2015;277(1):95–103. doi:10.1148/radiol.2015141856
225. Coupal TM, Mallinson PI, Gershony SL, et al. Getting the Most From Your Dual-Energy Scanner: recognizing, Reducing, and Eliminating Artifacts. *AJR Am J Roentgenol.* 2016;206(1):119–128. doi:10.2214/AJR.14.13901
226. Angelovski G. What We Can Really Do with Bioresponsive MRI Contrast Agents. *Angew Chem Int Ed Engl.* 2016;55(25):7038–7046. doi:10.1002/anie.201510956
227. Mao X, Xu J, Cui H. Functional Nanoparticles for Magnetic Resonance Imaging. *Wiley Interdiscip Rev Nanomed Nanobiotechnol.* 2016;8(6):814–841. doi:10.1002/wnan.1400
228. Stephen ZR, Kievit FM, Zhang M. Magnetite Nanoparticles for Medical MR Imaging. *Mater Today Kidlington Engl.* 2011;14(7–8):330–338. doi:10.1016/S1369-7021(11)70163-8
229. Ni D, Bu W, Ehlerding EB, Cai W, Shi J. Engineering of inorganic nanoparticles as magnetic resonance imaging contrast agents. *Chem Soc Rev.* 2017;46(23):7438–7468. doi:10.1039/c7cs00316a
230. Rogosnitzky M, Branch S. Gadolinium-based contrast agent toxicity: a review of known and proposed mechanisms. *Biometals Int J Role Met Ions Biol Biochem Med.* 2016;29(3):365–376. doi:10.1007/s10534-016-9931-7
231. Huang CH, Tsourkas A. Gd-based macromolecules and nanoparticles as magnetic resonance contrast agents for molecular imaging. *Curr Top Med Chem.* 2013;13(4):411–421. doi:10.2174/1568026611313040002
232. Thorek DLJ, Chen AK, Czupryna J, Tsourkas A. Superparamagnetic iron oxide nanoparticle probes for molecular imaging. *Ann Biomed Eng.* 2006;34(1):23–38. doi:10.1007/s10439-005-9002-7
233. Arami H, Khandhar AP, Tomitaka A, et al. In vivo multimodal magnetic particle imaging (MPI) with tailored magneto/optical contrast agents. *Biomaterials.* 2015;52:251–261. doi:10.1016/j.biomaterials.2015.02.040
234. Han Y, Zhou X, Qian Y, et al. Hypoxia-targeting dendritic MRI contrast agent based on internally hydroxy dendrimer for tumor imaging. *Biomaterials.* 2019;213:119195. doi:10.1016/j.biomaterials.2019.05.006
235. Liu X, Madhankumar AB, Miller PA, et al. MRI contrast agent for targeting glioma: interleukin-13 labeled liposome encapsulating gadolinium-DTPA. *Neuro-Oncol.* 2016;18(5):691–699. doi:10.1093/neuonc/nov263
236. Pagoto A, Stefania R, Garello F, et al. Paramagnetic Phospholipid-Based Micelles Targeting VCAM-1 Receptors for MRI Visualization of Inflammation. *Bioconjug Chem.* 2016;27(8):1921–1930. doi:10.1021/acs.bioconjchem.6b00308
237. Lin J, Chen X, Huang P. Graphene-based nanomaterials for bioimaging. *Adv Drug Deliv Rev.* 2016;105(Pt B):242–254. doi:10.1016/j.addr.2016.05.013
238. Vivero-Escoto JL, Huxford-Phillips RC, Lin W. Silica-based nanoprobe for biomedical imaging and theranostic applications. *Chem Soc Rev.* 2012;41(7):2673–2685. doi:10.1039/c2cs15229k
239. Loh KP, Ho D, Chiu GNC, Leong DT, Pastorin G, Chow EKH. Clinical Applications of Carbon Nanomaterials in Diagnostics and Therapy. *Adv Mater Deerfield Beach Fla.* 2018;30(47):e1802368. doi:10.1002/adma.201802368
240. Kobayashi H, Saga T, Kawamoto S, et al. Dynamic micro-magnetic resonance imaging of liver micrometastasis in mice with a novel liver macromolecular magnetic resonance contrast agent DAB-Am64-(1B4M-Gd)(64). *Cancer Res.* 2001;61(13):4966–4970.
241. Yan H, Gao X, Zhang Y, et al. Imaging Tiny Hepatic Tumor Xenografts via Endoglin-Targeted Paramagnetic/Optical Nanoprobe. *ACS Appl Mater Interfaces.* 2018;10(20):17047–17057. doi:10.1021/acsami.8b02648
242. Wang H, Ding W, Peng L, et al. Gadolinium-Loaded Solid Lipid Nanoparticles for Colorectal Tumor in MR Colonography. *J Biomed Nanotechnol.* 2020;16(5):594–602. doi:10.1166/jbn.2020.2922
243. Ding B, Zheng P, Ma P, Lin J. Manganese Oxide Nanomaterials: synthesis, Properties, and Theranostic Applications. *Adv Mater.* 2020;32(10):1905823. doi:10.1002/adma.201905823
244. Revia RA, Zhang M. Magnetite nanoparticles for cancer diagnosis, treatment, and treatment monitoring: recent advances. *Mater Today Kidlington Engl.* 2016;19(3):157–168. doi:10.1016/j.mattod.2015.08.022
245. An K, Kwon SG, Park M, et al. Synthesis of uniform hollow oxide nanoparticles through nanoscale acid etching. *Nano Lett.* 2008;8(12):4252–4258. doi:10.1021/nl8019467
246. Yang L, Wang L, Huang G, et al. Improving the sensitivity of T1 contrast-enhanced MRI and sensitive diagnosing tumors with ultralow doses of MnO octahedrons. *Theranostics.* 2021;11(14):6966–6982. doi:10.7150/thno.59096
247. Wei R, Gong X, Lin H, et al. Versatile Octapod-Shaped Hollow Porous Manganese(II) Oxide Nanoplatforam for Real-Time Visualization of Cargo Delivery. *Nano Lett.* 2019;19(8):5394–5402. doi:10.1021/acs.nanolett.9b01900
248. Wang YXJ. Superparamagnetic iron oxide based MRI contrast agents: current status of clinical application. *Quant Imaging Med Surg.* 2011;1(1):35–40. doi:10.3978/j.issn.2223-4292.2011.08.03

249. Huang J, Zhong X, Wang L, Yang L, Mao H. Improving the magnetic resonance imaging contrast and detection methods with engineered magnetic nanoparticles. *Theranostics*. 2012;2(1):86–102. doi:10.7150/thno.4006
250. Nishimura H, Tanigawa N, Hiramatsu M, Tatsumi Y, Matsuki M, Narabayashi I. Preoperative Esophageal Cancer Staging: magnetic Resonance Imaging of Lymph Node with Ferumoxtran-10, an Ultrasmall Superparamagnetic Iron Oxide. *J Am Coll Surg*. 2006;202(4):604–611. doi:10.1016/j.jamcollsurg.2005.12.004
251. Kim T, Cho EJ, Chae Y, et al. Urchin-shaped manganese oxide nanoparticles as pH-responsive activatable T1 contrast agents for magnetic resonance imaging. *Angew Chem Int Ed Engl*. 2011;50(45):10589–10593. doi:10.1002/anie.201103108
252. Ye D, Shuhendler AJ, Pandit P, et al. Caspase-responsive smart gadolinium-based contrast agent for magnetic resonance imaging of drug-induced apoptosis. *Chem Sci*. 2014;4(10):3845–3852. doi:10.1039/C4SC01392A
253. Lee GY, Qian WP, Wang L, et al. Theranostic nanoparticles with controlled release of gemcitabine for targeted therapy and MRI of pancreatic cancer. *ACS Nano*. 2013;7(3):2078–2089. doi:10.1021/nn3043463
254. Bor R, Fábíán A, Szepes Z. Role of ultrasound in colorectal diseases. *World J Gastroenterol*. 2016;22(43):9477–9487. doi:10.3748/wjg.v22.i43.9477
255. Shriki J. Ultrasound physics. *Crit Care Clin*. 2014;30(1):1–24, v. doi:10.1016/j.ccc.2013.08.004
256. Hu Y, Wang Y, Jiang J, et al. Preparation and Characterization of Novel Perfluorooctyl Bromide Nanoparticle as Ultrasound Contrast Agent via Layer-by-Layer Self-Assembly for Folate-Receptor-Mediated Tumor Imaging. *BioMed Res Int*. 2016;2016:6381464. doi:10.1155/2016/6381464
257. Theek B, Gremse F, Kunjachan S, et al. Characterizing EPR-mediated passive drug targeting using contrast-enhanced functional ultrasound imaging. *J Control Release off J Control Release Soc*. 2014;182:83–89. doi:10.1016/j.jconrel.2014.03.007
258. Lutz AM, Bachawal SV, Drescher CW, Pysz MA, Willmann JK, Gambhir SS. Ultrasound molecular imaging in a human CD276 expression-modulated murine ovarian cancer model. *Clin Cancer Res off J Am Assoc Cancer Res*. 2014;20(5):1313–1322. doi:10.1158/1078-0432.CCR-13-1642
259. Reinemann C, Strehlitz B. Aptamer-modified nanoparticles and their use in cancer diagnostics and treatment. *Swiss Med Wkly*. 2014;144:w13908. doi:10.4414/sm.w.2014.13908
260. Yin T, Wang P, Zheng R, et al. Nanobubbles for enhanced ultrasound imaging of tumors. *Int J Nanomedicine*. 2012;7:895–904. doi:10.2147/IJN.S28830
261. Min HS, Son S, You DG, et al. Chemical gas-generating nanoparticles for tumor-targeted ultrasound imaging and ultrasound-triggered drug delivery. *Biomaterials*. 2016;108:57–70. doi:10.1016/j.biomaterials.2016.08.049
262. Yang F, Wang Q, Gu Z, Fang K, Marriott G, Gu N. Silver nanoparticle-embedded microbubble as a dual-mode ultrasound and optical imaging probe. *ACS Appl Mater Interfaces*. 2013;5(18):9217–9223. doi:10.1021/am4029747
263. Ma M, Xu H, Chen H, et al. A drug-perfluorocarbon nanoemulsion with an ultrathin silica coating for the synergistic effect of chemotherapy and ablation by high-intensity focused ultrasound. *Adv Mater Deerfield Beach Fla*. 2014;26(43):7378–7385. doi:10.1002/adma.201402969
264. Wang CW, Yang SP, Hu H, Du J, Li FH. Synthesis, characterization and in vitro and in vivo investigation of C<sub>2</sub>F<sub>6</sub>-filled poly(lactic-co-glycolic acid) nanoparticles as an ultrasound contrast agent. *Mol Med Rep*. 2015;11(3):1885–1890. doi:10.3892/mmr.2014.2938
265. Park SH, Yoon YI, Moon H, et al. Development of a novel microbubble-liposome complex conjugated with peptide ligands targeting IL4R on brain tumor cells. *Oncol Rep*. 2016;36(1):131–136. doi:10.3892/or.2016.4836
266. Chen F, Ma M, Wang J, et al. Exosome-like silica nanoparticles: a novel ultrasound contrast agent for stem cell imaging. *Nanoscale*. 2017;9(1):402–411. doi:10.1039/c6nr08177k
267. Li H, Wang P, Wang X, et al. Perfluorooctyl bromide traces self-assembled with polymeric nanovesicles for blood pool ultrasound imaging. *Biomater Sci*. 2016;4(6):979–988. doi:10.1039/c6bm00080k
268. Caltagirone C, Bettoschi A, Garau A, Montis R. Silica-based nanoparticles: a versatile tool for the development of efficient imaging agents. *Chem Soc Rev*. 2015;44(14):4645–4671. doi:10.1039/c4cs00270a
269. Kitano M, Sakamoto H, Kudo M. Contrast-enhanced endoscopic ultrasound. *Dig Endosc off J Jpn Gastroenterol Endosc Soc*. 2014;26(Suppl 1):79–85. doi:10.1111/den.12179
270. Maghsoudinia F, Tavakoli MB, Samani RK, et al. Folic acid-functionalized gadolinium-loaded phase transition nanodroplets for dual-modal ultrasound/magnetic resonance imaging of hepatocellular carcinoma. *Talanta*. 2021;228:122245. doi:10.1016/j.talanta.2021.122245
271. VanOsdol J, Ektate K, Ramasamy S, et al. Sequential HIFU heating and nanobubble encapsulation provide efficient drug penetration from stealth and temperature sensitive liposomes in colon cancer. *J Control Release off J Control Release Soc*. 2017;247:55–63. doi:10.1016/j.jconrel.2016.12.033
272. Chen S, Xu XL, Zhou B, Tian J, Luo BM, Zhang LM. Acidic pH-Activated Gas-Generating Nanoparticles with Pullulan Decorating for Hepatoma-Targeted Ultrasound Imaging. *ACS Appl Mater Interfaces*. 2019;11(25):22194–22205. doi:10.1021/acsami.9b06745
273. Go Y, Lee H, Jeong L, et al. Acid-triggered echogenic nanoparticles for contrast-enhanced ultrasound imaging and therapy of acute liver failure. *Biomaterials*. 2018;186:22–30. doi:10.1016/j.biomaterials.2018.09.034
274. Mankoff DA, Bellon JR. Positron-emission tomographic imaging of cancer: glucose metabolism and beyond. *Semin Radiat Oncol*. 2001;11(1):16–27. doi:10.1053/srao.2001.18100
275. Li Z, Conti PS. Radiopharmaceutical chemistry for positron emission tomography. *Adv Drug Deliv Rev*. 2010;62(11):1031–1051. doi:10.1016/j.addr.2010.09.007
276. Miller PW, Long NJ, Vilar R, Gee AD. Synthesis of <sup>11</sup>C, <sup>18</sup>F, <sup>15</sup>O, and <sup>13</sup>N radiolabels for positron emission tomography. *Angew Chem Int Ed Engl*. 2008;47(47):8998–9033. doi:10.1002/anie.200800222
277. Saleem A, Charnley N, Price P. Clinical molecular imaging with positron emission tomography. *Eur J Cancer Oxf Engl*. 2006;42(12):1720–1727. doi:10.1016/j.ejca.2006.02.021
278. Larson SM. Positron emission tomography-based molecular imaging in human cancer: exploring the link between hypoxia and accelerated glucose metabolism. *Clin Cancer Res off J Am Assoc Cancer Res*. 2004;10(7):2203–2204. doi:10.1158/1078-0432.ccr-0002-4
279. Maffione AM, Rubello D, Caroli P, Colletti PM, Matteucci F. Is It Time to Introduce PET/CT in Colon Cancer Guidelines? *Clin Nucl Med*. 2020;45(7):525–530. doi:10.1097/RLU.00000000000003076
280. Freise AC, Zettlitz KA, Salazar FB, et al. Immuno-PET in Inflammatory Bowel Disease: imaging CD4-Positive T Cells in a Murine Model of Colitis. *J Nucl Med*. 2018;59(6):980–985. doi:10.2967/jnumed.117.199075

281. Low HY, Yang CT, Xia B, He T, Lam WWC, Ng DCE. Radiolabeled Liposomes for Nuclear Imaging Probes. *Molecules*. 2023;28(9):3798. doi:10.3390/molecules28093798
282. Garrigue P, Tang J, Ding L, et al. Self-assembling supramolecular dendrimer nanosystem for PET imaging of tumors. *Proc Natl Acad Sci U S A*. 2018;115(45):11454–11459. doi:10.1073/pnas.1812938115
283. Jensen AI, Binderup T, Kjaer A, Rasmussen PH, Andresen TL. Positron emission tomography based analysis of long-circulating cross-linked triblock polymeric micelles in a U87MG mouse xenograft model and comparison of DOTA and CB-TE2A as chelators of copper-64. *Biomacromolecules*. 2014;15(5):1625–1633. doi:10.1021/bm401871w
284. Huang G, Zhao T, Wang C, et al. PET imaging of occult tumours by temporal integration of tumour-acidosis signals from pH-sensitive <sup>64</sup>Cu-labelled polymers. *Nat Biomed Eng*. 2020;4(3):314–324. doi:10.1038/s41551-019-0416-1
285. Dearing JL, Park EJ, Dunning P, et al. Detection of intestinal inflammation by MicroPET imaging using a (64)Cu-labeled anti-beta(7) integrin antibody. *Inflamm Bowel Dis*. 2010;16(9):1458–1466. doi:10.1002/ibd.21231
286. Kim S, Chae MK, Yim MS, et al. Hybrid PET/MR imaging of tumors using an oleonic acid-conjugated nanoparticle. *Biomaterials*. 2013;34(33):8114–8121. doi:10.1016/j.biomaterials.2013.07.078
287. Li DF, Yang MF, Xu J, et al. Extracellular Vesicles: the Next Generation Theranostic Nanomedicine for Inflammatory Bowel Disease. *Int J Nanomedicine*. 2022;17:3893–3911. doi:10.2147/IJN.S370784
288. Liang Y, Duan L, Lu J, Xia J. Engineering exosomes for targeted drug delivery. *Theranostics*. 2021;11(7):3183–3195. doi:10.7150/thno.52570
289. Liu Q, Huang J, Xia J, Liang Y, Li G. Tracking tools of extracellular vesicles for biomedical research. *Front Bioeng Biotechnol*. 2022;10:943712. doi:10.3389/fbioe.2022.943712
290. Liang Y, Iqbal Z, Lu J, et al. Cell-derived nanovesicle-mediated drug delivery to the brain: principles and strategies for vesicle engineering. *Mol Ther J Am Soc Gene Ther*. 2023;31(5):1207–1224. doi:10.1016/j.ymthe.2022.10.008
291. Jing B, Qian R, Jiang D, et al. Extracellular vesicles-based pre-targeting strategy enables multi-modal imaging of orthotopic colon cancer and image-guided surgery. *J Nanobiotechnology*. 2021;19(1):151. doi:10.1186/s12951-021-00888-3
292. Aillon KL, Xie Y, El-Gendy N, Berkland CJ, Forrest ML. Effects of nanomaterial physicochemical properties on in vivo toxicity. *Adv Drug Deliv Rev*. 2009;61(6):457–466. doi:10.1016/j.addr.2009.03.010
293. Blanco E, Shen H, Ferrari M. Principles of nanoparticle design for overcoming biological barriers to drug delivery. *Nat Biotechnol*. 2015;33(9):941–951. doi:10.1038/nbt.3330
294. Zalba S, Ten Hagen TLM, Burgui C, Garrido MJ. Stealth nanoparticles in oncology: facing the PEG dilemma. *J Control Release off J Control Release Soc*. 2022;351:22–36. doi:10.1016/j.jconrel.2022.09.002
295. Song Q, Wang H, Yang J, et al. A “cluster bomb” oral drug delivery system to sequentially overcome the multiple absorption barriers. *Chin Chem Lett*. 2022;33(3):1577–1583. doi:10.1016/j.ccllet.2021.08.113
296. Ayer M, Klok HA. Cell-mediated delivery of synthetic nano- and microparticles. *J Control Release off J Control Release Soc*. 2017;259:92–104. doi:10.1016/j.jconrel.2017.01.048
297. Ostadhosseini F, Moitra P, Gunaseelan N, et al. Hitchhiking probiotic vectors to deliver ultra-small hafnia nanoparticles for “Color” gastrointestinal tract photon counting X-ray imaging. *Nanoscale Horiz*. 2022;7(5):533–542. doi:10.1039/d1nh00626f
298. Liu R, Luo C, Pang Z, et al. Advances of nanoparticles as drug delivery systems for disease diagnosis and treatment. *Chin Chem Lett*. 2023;34(2):107518. doi:10.1016/j.ccllet.2022.05.032

International Journal of Nanomedicine

Dovepress

## Publish your work in this journal

The International Journal of Nanomedicine is an international, peer-reviewed journal focusing on the application of nanotechnology in diagnostics, therapeutics, and drug delivery systems throughout the biomedical field. This journal is indexed on PubMed Central, MedLine, CAS, SciSearch®, Current Contents®/Clinical Medicine, Journal Citation Reports/Science Edition, EMBASE, Scopus and the Elsevier Bibliographic databases. The manuscript management system is completely online and includes a very quick and fair peer-review system, which is all easy to use. Visit <http://www.dovepress.com/testimonials.php> to read real quotes from published authors.

Submit your manuscript here: <https://www.dovepress.com/international-journal-of-nanomedicine-journal>